Master Degree Project

UNIVERSITY OF SKÖVDE

Utilization of Cancer-Specific Genome-Scale Metabolic Models in Pancreatic Ductal Adenocarcinomas for Biomarkers Discovery and Patient Stratification

Master Degree Project in Systems Biology A2E
60 credits/ECTS
Spring term 2019

Mohamed Al Shobky
a15mohel@student.his.se

Supervisor: Adil Mardinoglu,
Professor of Systems Biology
King's College London, UK
adil.mardinoglu@kcl.ac.uk

Examiner: Andreas Tilevik,
Senior Lecturer in Bioscience
School of Bioscience, Skovde university
andreas.tilevik@his.se

Abstract

Pancreatic Ductal Adenocarcinomas initiates in the exocrine part of the pancreatic tissue and represents over 90% of all the pancreatic cancers. Pancreatic Ductal Adenocarcinomas are extremely aggressive and are one of the most lethal malignant neoplasms. The five-year relative survival is currently less than 8% of the patients. The main reason behind such a low survival rate is that most of the cases are diagnosed at a very late stage. Although substantial advancement in pancreatic cancer research has been done, there has not been any remarkable significance in the mortality to incidence ratio. This is mainly a result of the scarce of early diagnostic characteristic symptoms and reliable biomarkers besides the unresponsiveness to the treatments. In this study, transcriptomics and proteomics data were used for the construction of a genome-scale metabolic model that was used in the detection of altered metabolic pathways, genes and metabolites using gene set analysis and reporter metabolites analysis. As a result, altered metabolic pathways in PDAC tumours were detected including the lipid metabolism-related pathways as well as carbohydrate metabolism, in addition to nucleotide metabolism, which are considered as potential candidates for diagnostic biomarkers.

Moreover, classification of the filtered DIRAC tightly regulated network genes, based on their prognostic values from the pathology atlas, detected two groups of PDAC patients that have a significantly different survival outcome. The differential expression analysis of the two groups showed that six of the eight genes used in clustering were showing significantly altered expression, which suggests their importance in PDAC patient stratification. As a conclusion, this study shows the valuable outcome of the GEM reconstructions and other systems-level analyses for elucidating the underlying altered metabolic mechanisms of PDAC. Such analyses results should provide more insights into the biomarker discovery and developing of potential treatments.

Popular scientific abstract

Cancer is a collective term for a large group of diseases that target any organ in the body. A well-known feature of cancer is its ability to create abnormal cells rapidly and grow outside their normal boundaries, which can then invade adjacent body parts and spread to distant organs. These abnormalities occur due to the interactions between the individual's genetic factors and external agents, including physical, chemical, and biological carcinogens. To give indications on cancer hazardousness, it is the second leading cause of death worldwide, with an estimated 9.6 million deaths in 2018, according to the world health organisation (WHO). Furthermore, the most common cancer types include the lung, breast, colorectal, prostate, skin, and stomach cancers and the lung, colorectal, stomach, liver and breast cancers are the most associated with cancer deaths. The cancer cell metabolism was found to be reprogrammed in order to support their rapid proliferation. That is why the metabolic rewiring, also referred to as metabolic alteration, is now considered as one of the cancer hallmarks that initially included the traits of evading growth suppressors, activating invasion and metastasis, limitless replicative potential, resisting cell death and sustained angiogenesis.

The pancreas is an organ located within the abdomen and is about 15.24 cm long, flat and oblong, with an essential rule in digestion and blood sugar regulation. The pancreas as a gland has both exocrine and endocrine functions. The exocrine activity is shown in the production of enzymes called pancreatic juice that digest fats, proteins and carbohydrates in the intestine. Those digestive fluids travel through the pancreatic duct to the bile duct that takes the fluids to the gallbladder and mixes with bile acid to help in the digestion process. The endocrine activity is the represented in its secretion to the insulin that decreases the concentration of blood glucose and glucagon raises the blood glucose levels, and the combination of the two hormones maintain a normal level of blood sugar in the human body. There are three primary diseases associated with the pancreas malfunction, and they are pancreatitis, diabetes and pancreatic cancer. The pancreatic ductal adenocarcinoma is a highly lethal cancer associated with a very poor survival rate as the five-year relative survival is currently less than 8% of the patients. The cytotoxic chemotherapies that are now being used in the treatment regimen, unfortunately, are accompanied by significant side effects with a minimal therapeutic outcome. The FDA approved drugs that are used rely on the DNA metabolism and DNA integrity as their primary target, and for that reason, researchers thought of finding alternative metabolic targets that might allow for a higher efficacy and tumour eradication rate. Pancreatic ductal adenocarcinomas are capable of living in a harsh microenvironment with hypoxia and nutrient deprivation, which means that they attain biochemical flexibility, allowing them to adapt in such conditions. For that reason, a full understanding of the metabolic nature can ravel metabolic vulnerabilities that could be targeted as biomarkers for diagnoses or prognosis and as a novel drug target for developing an effective treatment. In this study, different systems biology methods including genome-scale metabolic modelling, differential expression analysis, gene set enrichment analysis, survival analysis and more were used to detect genetic and metabolic alterations specific to pancreatic cancer. The results revealed that pancreatic tumours possess altered metabolism in the lipid metabolism, carbohydrate metabolism as well as nucleotide metabolism pathways that can be targeted as potential candidates of diagnostic biomarkers. In addition, the analysis managed to detect a list of 6 genes that have altered expression between patient groups suggesting their importance in pancreatic patient stratification which can help in determining the cancer stage and the subsequent adequate and effective treatment.

List of abbreviation

AADAC	Arylacetamide deacetylase
ALDH3A1	Aldehyde dehydrogenase 3 family member A1
CHI3L1	Chitinase-3-like protein 1
DEGs	Differentially expressed genes
DIRAC	Differential Rank Conservation
ENTPD8	Ectonucleoside Triphosphate diphosphohydrolase 8
FPKM	Fragments Per Kilobase of transcript per Million mapped reads
GDC	Genomic Data Commons
GEM	Genome-scale metabolic model
GFPT1	Glutamine--fructose-6-phosphate aminotransferase
GSA	Gene set analysis
HK3	Hexokinase-3
HMR2	Human Metabolic Reaction database 2
HPA	The Human Protein Atlas
LDHA	L-lactate dehydrogenase A chain
MANSC 1	MANSC domain-containing protein 1
MOGAT2	Monoacylglycerol O-acyltransferase 2
MOGAT3	Monoacylglycerol O-acyltransferase 3
NAGK	N-acetyl-D-glucosamine kinase
PDAC	Pancreatic Ductal Adenocarcinoma.
PLA2G10	Phospholipase A2 Group IVF
PLA2G4F	phospholipase A2 group X
TCGA	The Cancer Genome Atlas
tINIT	Task-driven Integrative Network Inference for Tissues

Table of contents

Introduction

As the fundamental building unit of the human body, cells are capable of both extracting and providing energy to carry out various vital processes and synthesising new organic materials that are essential for performing activates such as movement, growth, development, and reproduction. Metabolism is a crucial process for the utilisation of nutrients and preserving the balance between energy consumption and production by a collection of a set of biochemical reactions which in turn are maintaining the healthy living state of the cells and the body as a whole (Lazar and Birnbaum, 2012). With the mutual impact between the metabolism and every other cellular process; there is a piece of apparent evidence showing the fundamental role of the metabolic pathways collection that influences every single cellular function and extends to whole-body level (McKnight, 2010). To this end, along with a more profound medically-oriented research in metabolism, it became more evident that the abnormal metabolic states considered as the primary cause or outcome of a myriad of human disorders including diabetes, liver and renal disorders, and cancer (DeBerardinis and Thompson, 2012).

Cancer is a remarkably heterogeneous and sophisticated collection of diseases and considered as an outstanding example of human disorder with hereditarily-derived pathological metabolic perturbations (Greaves and Maley, 2012). Hanahan and Weinberg (Hanahan and Weinberg, 2000) managed to set six major cancer hallmarks in an attempt to organise the cancer discrepancy in its underlying biology that represents the physiological alteration in a cell which eventually drives the growth and development of the malignancy. Those hallmarks are represented in the tumour ability to generate its own growth signals, showing a noticeable reduction in its dependence on the exogenous growth stimulation from the surrounding normal tissue microenvironment. Another acquired trait by the tumour cells is the insensitivity to the antigrowth signals, which is mainly caused by the disruption of the retinoblastoma protein (pRb) and its two relatives, p107 and p130 that release E2F transcription factors that allow the cell proliferation. One more critical mechanism is the ability of the tumour cells to evade apoptosis that has a very prominent influence on the expansion of the tumour cell population that works side by side with its ability to increase the rate of cell proliferation by acquiring insensitivity to the antigrowth signals. Independent from the cell-to-cell signalling disruption in favour of tumour growth to be isolated from the surrounding environment, the deregulation of the intrinsic, cell-autonomous program that operates independently from the cell-to-cell signalling pathways, are crucial to ensure the uncontrolled expansion of the tumour growth. The availability of the oxygen and nutrients by the blood vessels to the tumour cells is also crucial to keep the tumour expansion and increase in size. For that particular reason, the tumour develops a sustained angiogenic ability that guarantees a constant supply from oxygen and nutrients. The last hallmark they introduced was the ability of the cancer cells to invade adjacent tissues and move to remote sites to start new colonies to escape from the limited supplies in the primary tumours.

Later an updated review by the same authors (Hanahan and Weinberg, 2011) added to the list two more emerging hallmarks based on observations from the significant advancement in cancer research and that included the of energy metabolism reprogramming and evading immune destruction. Metabolic reprogramming as a cancer hallmark has the capability to promote the malignant cell

proliferation, survival, and metastasis by altering metabolic pathways and mainly those related to energy metabolism, aiming for maintaining the cell growth and division. That was first observed by Warburg where cancer cells showed an abnormal behaviour from healthy cells in terms of energy metabolism (Warburg, 1956, Warburg et al., 1927). In other words, within aerobic conditions, the abnormal cells alter the metabolism of glucose where the energy metabolism is shifted mainly towards glycolysis in what so-called "aerobic glycolysis" (Warburg, 1956, Warburg et al., 1927). While that was such an outstanding discovery, but the idea of the total impairment of the oxidative phosphorylation process in cancer cells respiration was controversial (Weinhouse, 1956). That was supported by carrying out an isotope-tracing experiment that showed results of the ability of cancer cells to oxidise oxygen and generate CO2 with the same rate as a normal cell. The only exception was during tumour growth where the core cells of a tumour become hypoxic, and that would decrease the oxidative phosphorylation rate in comparison to glycolysis (Weinhouse, 1951, Weinhouse, 1972).

Recently, the tumour associated metabolic rewiring was intensely reviewed and showed its profound advantage to initiate the tumour growth and development as well as maintaining its survival. In addition to that, it became more evident that this metabolic reprogramming could be a result of genetic mutations or could even induce posttranscriptional modifications (DeBerardinis and Chandel, 2016, Cairns and Mak, 2016). In an attempt to organise these metabolic alterations, Pavlova and Thompson managed to group them into six hallmarks (Pavlova and Thompson, 2016). The list included the deregulation of the glucose and amino acids, increased nitrogen demand, the tumour utilisation for the opportunistic modes of nutrient acquisition and the ability to interact with its surrounding microenvironment metabolically. Moreover, the utilisation of the intermediates of the glycolysis\TCA cycle for the biosynthesis and NADPH production and alterations in metabolite-driven gene regulation that acts as active influencers on tumorigenesis were among those hallmarks (Pavlova and Thompson, 2016).

In general, pancreatic cancers can be divided into two subtypes as endocrine or exocrine tumours. Pancreatic Ductal Adenocarcinomas (PDAC) initiates in the exocrine part of the pancreatic tissue and represents over 90% of all the pancreatic cancers. The most typical non-invasive neoplastic precourse to PDAC is pancreatic intraepithelial neoplasias (PanIN). Those lesions harbour genetic and epigenetic alterations that are considered as primary drivers of the invasive adenocarcinoma of the pancreatic tissue (Vincent et al., 2011). PDACs are extremely aggressive, and one of the most lethal malignant neoplasms with five-year relative survival is currently less than 8% of the patients. The main reason behind such a low survival rate is that most of the cases are diagnosed at a very late stage, where the five-year rate of survival reaches 2% (Siegel et al., 2016). Based on GLOBOCAN 2012 worldwide estimates, the pancreatic cancer was responsible for the death of 330391 patients per year, accounting for 4.0% of all cancer deaths, and also 337872 per year estimated incidence which is accounting for 2.4% of all new cancer cases (Ferlay et al., 2015). With the fact that the PDAC considered the seventh most common cause of cancer mortality with an inferior prognosis, it is predicted that this cancer-related mortality rate is going to even more increase reaching to be ranked as second in the next decade if no actions will be taken against such deadly cancer (Rahib et al., 2014).

Although the substantial advancement in pancreatic cancer research there has not been any remarkable significance in the mortality to incidence ratio. That is mainly a result of the scarce of early diagnostic characteristic symptoms and reliable biomarkers besides the unresponsiveness to the

treatments due to the tumour heterogeneity, plasticity and the aggressive metastasis that presents in more than 50% of the diagnosed patients (Adamska et al., 2017). Previously, several studies pointed out the most prominent genetic features of the PDAC such as oncogenic activation of K-RAS that is a standard feature in more than 90% of the patients and with the early onset mutation of that gene, it is considered as a critical driver of PDAC initiation and progression (Lohr et al., 2005). Along with the oncogenic activation, inactivating mutations of the tumour suppressor gene CDKN2A/2B are also observed in more than 80% of the early stage lesions, while later stages of cancer exhibit inactivating mutations and deletions of tumour suppressor genes most prominently include TP53and SMAD4 (Bardeesy and DePinho, 2002). Moreover, another feature that reflects the PDAC aggressiveness and chemoresistance is the desmoplastic reactions induced by immune cells, stromal cells, neural cells and extracellular matrix that forms the tumour mass bulk. Altogether, with the tumour hypo vascularisation, the delivery of the needed oxygen and nutrients is diminished due to the vascular network deficiency. In such hypoxic and acidic microenvironment in addition to the nutrient deficiency, a direct impact on the drug delivery mechanisms is common, and more importantly, the tumour microenvironment maintains its survival and growth by altering its metabolism (Sousa and Kimmelman, 2014, Liang et al., 2016). The downstream events of metabolic reprogramming are considered as prominent hallmarks of PDAC. Therefore tackling this aggressive cancer through establishing a clear understanding regarding its metabolism has been a dominant challenge to the scientific and medical communities (Perera and Bardeesy, 2015). Recent studies have shown the crucial role of both glucose and glutamine metabolism in the progression of the PDAC tumours that are regulated by the K-RAS oncogene to maintain the tumour growth (Le et al., 2010, Ying et al., 2012, Son et al., 2013). Inducible oncogenic K-RAS mouse model of PDAC showed in addition to being a key driver of PDAC initiation that it plays a central role in rewiring the tumour glucose metabolism by stimulating the glucose uptake and drives glycolysis intermediates towards non-oxidative pentose phosphate pathways (PPP) (Ying et al., 2012). Another study reported that the PDAC cells maintain the tumour growth by relying on the distinct pathway of glutamine metabolism and that this reprogramming is mediated by the oncogenic K-RAS (Son et al., 2013).

One of the fundamental purposes of the human systems biology studies is to accomplish an explicit knowledge about human metabolism and its relation to various diseases. With the frequently arising challenges regarding cancer diagnosis and treatment - mainly due to its complex pathogenic landscape and cellular heterogeneity - the systems biology holistic view allowed for having a global understanding of the disease mechanism and gain more insight towards biomarkers and drug target discovery (Westerhoff and Palsson, 2004, Tian et al., 2012). Metabolic network reconstructions became an essential tool for exploring the systems biology of metabolism and the generation of genome-scale metabolic models (GEMs). These models along with the massive advancement in high-throughput omics data production has significantly contributed to metabolism studying on a genome-scale by providing a computational platform for integrating and analysing this data as well as investigating more thoroughly into these networks by simulations (Thiele and Palsson, 2010, Bordbar and Palsson, 2012, Fondi and Lio, 2015).

GEMs are a mathematical representation of the current knowledge of metabolism where biochemical and physiological data on protein-encoding genes and their interactions with other bioactive compounds and associated reactions are integrated. These metabolic reconstructions harbour a set of annotated stoichiometric chemical reactions as well as enzymes associated with those reactions in

a particular cell or tissue (Mardinoglu and Nielsen, 2012, Mardinoglu et al., 2013, Mardinoglu and Nielsen, 2015). In the past, two literature based GEMs of human metabolism were constructed, which were built to be generic. The reconstruction based on an extensive evaluation of genomic and bibliomic data, which are known as Recon1 (Duarte et al., 2007) and the Edinburg Human Metabolic Network (EHMN) (Ma et al., 2007), which showed a great significance in revealing the gaps in understanding the human metabolism. With the aim of extending the knowledge, included within such reconstructions, these generic networks were integrated with the human metabolism-related reactions in the Kyoto Encyclopaedia of Genes and Genomics (KEGG) (Kanehisa and Goto, 2000) for the creation of the Human Metabolic Reaction (HMR) database (Agren et al., 2012). This was followed by updating the contents of the HMR to HMR2 database (Mardinoglu et al., 2013) by integrating lipids and lipoprotein metabolomics from the Reactome database (Croft et al., 2011) and a manually constructed Hepatocytes GEM, HepatoNet 1 (Gille et al., 2010). Also, the lipid metabolism was more extensively curated using the lipidomics Gateway (Sud et al., 2007) and HumanCyc database (Romero et al., 2005). Those generic GEMs lack information related to the cell or disease-specific metabolic states. For that reason, many algorithms have been published that can reconstruct a cell or disease-specific GEM by reducing the generic ones using cell or diseases specific omics data (Schmidt et al., 2013).

By the time the Genome-Scale Metabolic network was reconstructed, it was ready to be paired with various constraint-based modelling approaches for its transformation to mathematical models for the analysis of the cell or tissue-specific genotype-phenotype relationships. Concerning the current network knowledge, the constraint-based modelling constrains its predications allowing for phenotype simulations (Price et al., 2004). The constraint-based modelling, in contrast to the traditional kinetic modelling techniques, does not need detailed information on kinetic constants or the associated metabolites and enzyme. Instead, it counts on a set of constraints including thermodynamic constraints, mass-balance constraints and enzyme capacity constraints that applied for analysing Genome-scale metabolic models by transforming it into a mathematical model (Lewis et al., 2012). For the purpose of genome-scale metabolism simulations, Flux Balance Analysis (FBA) considered as the primary and most common method of the constraint-based modelling, allows for *in silico* prediction of flux that is optimised to a defined set of objectives despite the need for experimental measurements (Orth et al., 2010). Cancer-related applications of the reconstructed GEMs includes networks comparison between healthy and diseased cells; physiological analysis including essentiality and lethality analysis and growth simulation; integrative analysis of omics data, in which the GEM is used as a scaffold for identifying reporter pathways and reporter metabolites (Yizhak et al., 2015, Nilsson and Nielsen, 2017, Ghaffari et al., 2015).

Aim

With the high heterogeneity, aggressiveness and low survival rates of pancreatic adenocarcinomas; early diagnosis along with appropriate personalised treatment protocols are crucial for tackling such lethal tumours. For that reason, this project aims to integrate the pancreatic cancer-specific proteomics and transcriptomics data with Genome-scale metabolic modelling in a systematic manner. Moreover, the aim is to perform transcriptomic and network-based analyses, as illustrated in figure 1, to discover potential biomarker candidates and stratify PDAC patients that eventually will be significant for the diagnosis and development of effective treatment strategies.

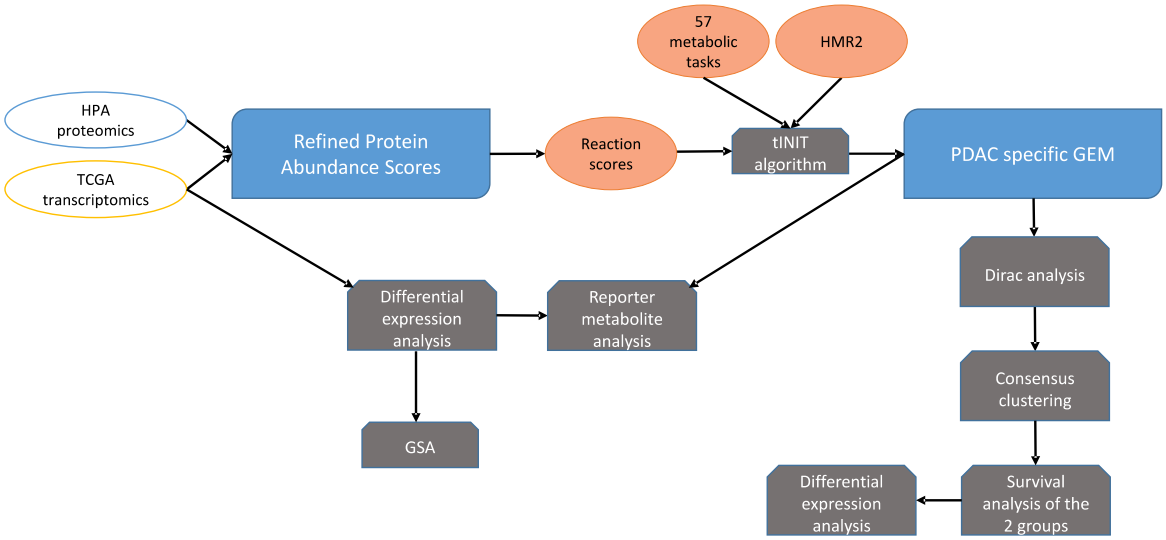

Figure 1. Illustration of the workflow of the thesis project. TCGA mRNA-seq data and HPA proteomics data were integrated and introduced to the tINIT algorithm along with 57 metabolic tasks and HMR2 as a template model for the reconstruction of PDAC-specific GEM. For the diagnostic biomarkers discovery, differential expression (DE) analysis was performed, and the results were used to perform gene set analysis (GSA) and reporter metabolites analysis using the network topology of the reconstructed GEM. For the PDAC patients' stratification, Differential Rank Conservation (DIRAC) analysis followed by consensus clustering analysis and survival analysis was performed. DE analysis was then performed between the two groups.

Materials and Methods

2.1 DATA

2.1.1 Proteomics

Staining profiles for proteins in pancreatic ductal adenocarcinomas tissue based on immunohistochemistry using tissue microarrays were retrieved from the Human Protein Atlas (HPA) version 16.1 (Uhlén et al., 2015) (http://www.proteinatlas.org). The proteomics data were used as the bases for the Genome-scale metabolic model reconstruction.

2.1.2 Transcriptomics

The mRNA-Seq profiles and clinical metadata of 181 samples composed of 177 primary pancreatic ductal adenocarcinomas and four matched tumour-adjacent normal tissues were used for the GEM reconstruction and mRNA expression, DIRAC, clustering and survival analyses. The harmonised data were retrieved from The Cancer Genome Atlas (TCGA) project within the Genomic Data Commons (GDC) Data Portal Version 9.0 (https://portal.gdc.cancer.gov/) (Grossman et al., 2016), using the TCGAbiolinks 2.5.7 R/Bioconductor package (Colaprico et al., 2016). The retrieved harmonised mRNA-Seq gene expression was in the form of raw HT-Seq Read Counts data, and Fragments per Kilobase of transcript per Million mapped reads (FPKM) data.

2.1.3 Generic human model, Human Metabolic Reaction database 2 (HMR2)

The reference human GEM HMR2 (Uhlen et al., 2017) is a genome-scale metabolic model that represents the generic human cell. It contains 2892 genes associated with 7762 reactions 5566 metabolites. The generic GEM was used as the reference model for the tINIT algorithm during the process of PDAC-specific GEM reconstruction.

2.2 The RAVEN Toolbox

RAVEN (Reconstruction, Analysis, and Visualization of Metabolic Networks) is a toolbox that runs within MATLAB and presents a complete environment to perform GEMs reconstruction, with the ability to analyse, simulate and visualise those reconstructed models. It is capable of integrating different omics data for automated reconstruction of the GEMs. The reconstruction was followed by an analysis of the networks and simulation results, also visualising the GEMs based on another published network maps (Agren et al., 2013).

2.3 PDAC-specific GEM Reconstruction

A functional PDAC-specific GEM was reconstructed based on both proteomic and transcriptomic data, using HMR2 as a reference model and a list of 57 predefined metabolic tasks (Agren et al., 2014) as an input to the tINIT (Task-driven Integrative Network Inference for Tissues) algorithm (Agren et al., 2014) and Mosek solver version 8 within the RAVEN Toolbox Version 1.9 in MATLAB R2016b. Scoring for evidence of a reaction to be occurring was based on HPA protein profiles integrated with mRNAseq FPKM data. mRNA-seq data were filtered using the criterion of median expression value ≥1 FPKM to be added to HPA protein abundance score file with the Level “Low”. Such reconstruction method was

performed in many projects; for example, one group integrated myocyte-specific RNA seq data with proteomic data for the reconstruction of a comprehensive myocyte-specific GEM (Varemo et al., 2015). The maximisation of biomass production was considered as an objective function for PDAC-specific GEM to assess model feasibility. In brief, the tINIT algorithm is a developed version from the older INIT (Agren et al., 2012) that allows for direct automated and semi-automated reconstruction of functional GEMs based on proteomics and transcriptomics evidence and a novel task-driven reconstruction approach. The INIT algorithm was also used for generating a cell or cancer-specific GEMs that were lacking the functionality to allow performing the simulations. On the other hand, tINIT takes as an input, in addition to the integrated proteomics and transcriptomics evidence score and a Generic model, a list of predefined metabolic tasks including biomass growth for cancer cells as an additional metabolic task. These tasks should be performed by the reconstructed model to be functional as they are applying constraints on the reconstruction functionality and representing metabolic functions that are common in all cell types (Agren et al., 2014).

2.4 The Differential Rank Conservation (DIRAC) analysis

DIRAC is a network-based approach and was implemented within MATLAB for analysing gene order within the pathways of the reconstructed model along with another gene sets. The central concept of the algorithm is mainly based on the relative expression ranks of the participating genes. The results should show a quantitative measurement of how pathway rankings differ both within and between phenotypes (Eddy et al., 2010). Pathways of the reconstructed GEM, as well as KEGG pathways, were used as gene set input to the algorithm with minimum genes set size was set to 3 and FPKMs were filtered by removing genes that had a row median less than one.

2.5 Unsupervised clustering

To find hidden patterns in the transcriptomics data that could be used for the PDAC stratification, unsupervised class discovery using the R/Bioconductor package "ConsensusClusterPlus" has proven its efficacy in revealing those groups that share common biological characteristics (Wilkerson and Hayes, 2010). First, the transcriptomics data in the form of FPKMs were filtered based on median FPKM > one will be included. Then, the list of 152 unique genes from the four tightly regulated pathways was further filtered based on their significance as prognostic genes from the pathology atlas dataset of pancreatic cancer prognostic genes (Uhlen et al., 2017). The FPKMs were median centred, and the following parameters were used: 80% item resampling (pItem), and 80% gene resampling (pFeature), a maximum evaluated k of 12 and 1000 resampling, agglomerative hierarchical clustering algorithm (clustering) upon 1- spearman correlation distances (distance) and ward.D2 as the linkage method.

2.6 Survival analysis

Based on the clinical data from the TCGA of the two PDAC groups defined by the unsupervised consensus clustering, the survival analysis was performed, and the log-rank test was calculated. Kaplan-Meier curves were derived according to the survival of the patients, and the days occurred until death after diagnosis. The Survival R package (Therneau and Lumley, 2018) was used for this analysis.

2.7 Differential Gene expression analysis and gene set analysis (GSA)

The mRNA-seq raw count data were analysed for the detection of differentially expressed genes (DEGs) and obtain a quantitative and statistical inference to the changes between the two conditions as well as between the generated cancer subgroups from clustering. The R/Bioconductor package DESeq2 version 1.18.1 (Love et al., 2014) was used for that purpose. Benjamini and Hochberg false discovery rate (FDR) was conducted for multiple hypothesis correction. The FDR adjusted p-value < 0.05 and Fold-change cut-off of >1 or <-1 was applied to determine up- and down-regulated genes.

Gene set analysis using R/Bioconductor package "Piano" (Varemo et al., 2013), was performed to gain a better understanding to the results of the differential expression analysis, and its underlying biological processes. In this study, three gene set collections including the constructed PDAC specific GEM, the Gene Ontology biological processes (BP) "GOTERM_BP_5" and KEGG metabolic pathways (both were retrieved from MSigDB (Liberzon et al., 2015) were used. The statistical GSA method used was: Reporter features, Theoretical null distribution as the Significance method, FDR as the Multiple hypothesis correction method <0.05 and 1000 permutations to use for gene sampling

2.8 Reporter metabolites

By using the network topology of the reconstructed model, the reporter metabolite algorithm impeded inside the RAVEN toolbox was employed to allow for identifying the network metabolites that are significantly enriched based on its association with the gene expression changes. Those metabolites can be then used for identifying central parts of the metabolic network that has significant perturbation between the examined conditions (Patil and Nielsen, 2005). The network topology of the reconstructed PDAC-specific GEM in addition to the log2 fold changes and p-values from the differential expression analysis were imported to the *reporter metabolites* function in the RAVEN toolbox and a p-value < 0.005 was determed as the significance level.

Results

3.1 Integrated proteomics and transcriptomics data for a refined protein abundance scores

The concept behind integrating both of the proteomics and transcriptomics data is to complement the proteomics data and get a piece of refined and more robust information that could overcome the heterogeneous nature of pancreatic cancer tumours. The protein level data serves as the main source of protein evidence, while the mRNA expression profiles purpose is to fill in the gaps and reduce the probability of having potential false negatives.

The retrieved PDAC proteomics data from the HPA project v16.1 was trimmed down to show the protein abundance levels (high, medium, low or not detected) of 15297 protein-encoding genes that are associated with the highest patients count. As a result, the data unveiled that 1566 (10.2%) genes had high staining level, 1835 (12%) genes had low staining level, 5368 (35.1%) genes had medium staining level, while 6528 (42.7%) genes were not detected on the protein level (Figure 2A).

The TCGA transcriptomics data for 177 PDAC patients and four matched tumour-adjacent normal tissues in the form of FPKMs were filtered to comprise only protein-encoding genes, and that yielded in total 19363 putative protein-coding genes. Based on various studies of the correlation between transcriptome and proteome, the low abundance transcripts of the mRNA expression with median FPKM values less than one was interpreted as not being translated to the corresponding proteins (Fagerberg et al., 2014, Varemo et al., 2015). By applying a cut-off of median FPKM equal to or above one as the protein detection level, a total of 12134 (62.7%) were identified as detected, while 7229 (37.3%) of the putative protein-coding genes were not being translated to their corresponding protein (Figure 2B).

Besides, comparing the two datasets revealed that a total of 6890 (49.2% of all protein-coding genes) genes were consistently present in PDAC tumours at both the proteomic and transcriptomic levels (Figure 2C). Moreover, a total of 5244 (37.4%) protein-coding genes were unique to the transcriptomic data, while 1879 (13.4%) protein-coding genes were only present in the proteomics data (Figure 2C). With that being concluded, the integrated data represented all the protein-coding genes (14013 genes) that are evaluated as present on the protein level in PDAC tumours. Based on this, 3557 genes from the HPA data with non-detected protein abundance level but had an FPKM level more than or equal to one were reassigned as detected with low level. In addition, 1687 genes were absent from the HPA data and found to have an FPKM level more than or equal to one. These genes were also added to the final updated protein abundance scores with the level defined as low.

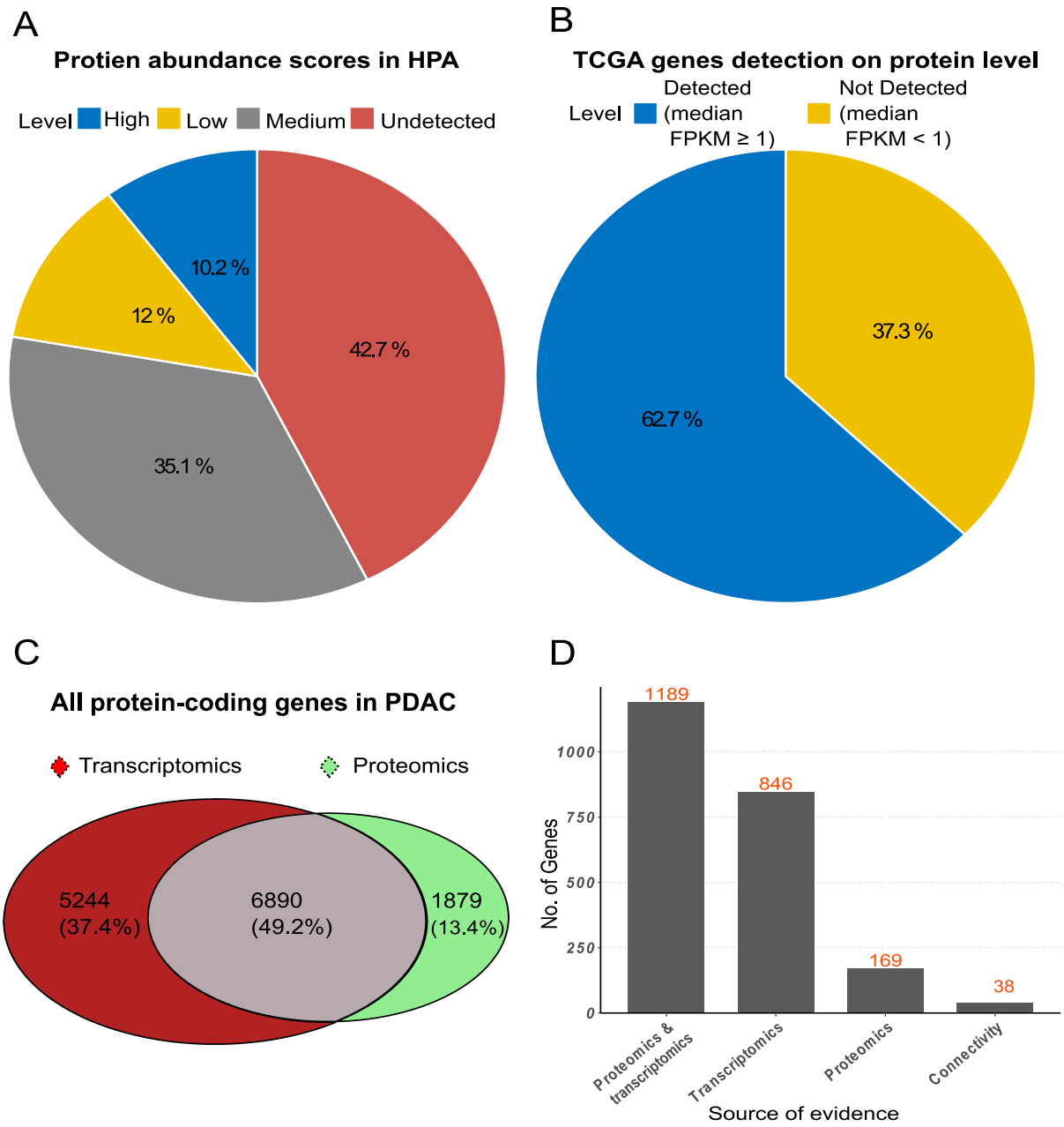

Figure 2: Coverage of gene expression in transcriptomic and proteomic analysis of the PDAC data. (A) The pie chart shows the coverage of protein-coding genes in the Human Protein Atlas (HPA). (B) The pie chart shows the coverage of protein-coding genes in the TCGA FPKM data after applying the median cutoff FPKM <1. (C) All protein-coding genes that are evaluated as present in PDAC based on TCGA transcriptomics data (Red) and HPA proteomics data (Green), which were used during the reconstruction of the PDAC GEM. (D) The overall distribution of Genes in PDAC GEM are included in the model based on the high-quality proteome, transcriptome, as well as the connectivity.

3.2 Reconstructed PDAC-specific GEM constitutes individual transcriptome and tissue-specific proteome data

The high heterogeneity is a prominent trait of the pancreatic ductal adenocarcinoma tumours that obstruct the process of detecting individual variations within the tumours and the global biological differences between cancerous and non-cancerous pancreatic tissues. In this context, a population-based PDAC-specific GEM was reconstructed that comprise the individual variations among the PDAC

tumours and can be further employed for analysing high throughput omics data and simulating the metabolic differences between cancer and healthy patients.

The reconstruction process mainly relied on the updated protein abundance levels that were generated from the integration of both the proteomics and transcriptomics data (Figure 2C) and used to score the HMR2 reactions to be included in the reconstruction if at least one of its associated genes was detected as present in PDAC tumours. The model functionality was determined based on the 57 metabolic tasks and the objective function (see methods), and as a result, 459 reactions associated with 492 genes were essential for performing the introduced biological tasks. In addition, the final gap-filling step added eleven reactions that allow the final model to perform the rest of the tasks. The resulting PDAC- specific GEM is a functional model including 5750 reactions associated with 2242 genes and 4415 metabolites within eight different subcellular compartments. By inspecting the gene content of the reconstructed model and its correlation with the introduced proteomics and transcriptomics data, it showed that the majority of model gene content (1189 genes) were derived from both of the –omics data, while a considerable number (846 genes) of genes were specific to the transcriptomics data and only 169 genes were unique to the HPA proteomics data. In addition, a few numbers of genes (38 genes) were found to be included in the model from the HMR2 database for enhancing the model connectivity (Table Appendix .1). The source of evidence for the GEM gene content is shown in Figure 2D**.**

3.3 RNA-seq and Network-based analyses of PDAC metabolism

In order to uncover the underlying biological differences between PDAC tumours and noncancerous pancreatic tissues, transcriptomics data were analysed for the identification of the differentially expressed genes (DEGs) using the DEseq 2 R package (Love et al., 2014). As a result, a total of 540 genes were found to be differentially expressed (FDR adj. p-value < 0.05) in primary tumours in comparison to non-cancerous pancreatic tissue, of which 305 genes were upregulated, and 235 genes were downregulated. A complete list of all the 540 genes that were differentially expressed is shown in table Appendix 2.

The results of the differential expression analysis (more specifically the log-fold changes along with the p-values) for the protein-coding genes were used to perform gene set analysis (GSA) for Gene Ontology biological processes (BP) "GOTERM_BP_5", KEGG metabolic pathways and the network structure of the PDAC-specific GEM using the Piano R/Bioconductor package (Varemo et al., 2013). The results for the GO biological processes gene set analysis showed that 584 biological processes were associated with upregulated genes in PDAC while 379 were associated with downregulated genes in PDAC. Among the significantly upregulated processes are mitotic cell cycle, cell cycle process, cell division, DNA replication, DNA repair, DNA metabolic process, cellular respiration, cytoplasmic translation and cell development. Also several metabolic processes including oxidative phosphorylation, one carbon metabolic process, carbohydrate metabolic and biosynthetic processes, amino acid metabolic processes including aspartate and glutamate metabolism, extensive lipid metabolic and biosynthetic processes like arachidonic acid, fatty acid, fatty acid derivatives, steroids and ether metabolic processes. Whereas immune-related biological processes, such as activation of immune response, inflammatory response, alpha and beta T-cell activation and differentiation, macrophage activation and cellular defence response, were associated with significantly downregulated genes in PDAC.

In the same manner, results of gene set analysis for both KEGG pathways and PDAC-specific GEM subsystems showed similar significance levels (FDR adj.pval<0.05) for the perturbed gene sets. The former resulted in 27 pathways showing patterns of downregulation due to its association to downregulated genes while 40 pathways were enriched by upregulated genes; the later showed that 35 subsystems were associated with upregulated genes and none of the rest subsystems found to be significantly enriched with downregulated genes. Noticeably, pathways including type 1 diabetes mellitus, primary immunodeficiency, natural killer cell mediated cytotoxicity, T cell receptor signalling, B cell receptor signalling, chemokine signalling, jak stat signalling, neurotrophin signalling autoimmune thyroid disease and acute myeloid leukaemia were among the highly significantly KEGG pathways enriched with downregulated genes. Moreover, the results showed that among the highly enriched metabolic pathways with upregulated genes are the lipid metabolism pathways including arachidonic acid, acylglycerides, glycerophospholipid, steroid, ether, glycosphingolipid metabolisms and bile acid biosynthesis and recycling. In addition, it comes in the same category as the amino acid metabolism pathways such as alanine, aspartate and glutamate metabolism, glycine, serine and threonine metabolism, cysteine and methionine metabolism, and arginine and proline metabolism.

Along with that energy metabolism related pathways such as oxidative phosphorylation as well as carbohydrate, nucleotide and cofactors and vitamins metabolism pathways were also among the highly enriched with upregulated genes. Those pathways are shown in details in table 1, along with the associated differentially expressed genes for each pathway. Noticeably, although most of the genes were showing upregulated expression in PDAC tumours, a small amount of them was found to be downregulated, which did not affect the overall outcome.

Table1: Common significant Pathways (padj<0.05) identified through DE and "PIANO" GSA analyses (based on KEGG and/or PDAC GEM), as well as significantly changed genes in each pathway. The genes of each pathway are arranged by the degree of significance of differential expression within each pathway. The gene symbol, the log2 fold change, LFC standard error, p-values, and FDR adj. p-values are presented for each gene. Genes in (Red) are downregulated genes in PDAC.

Metabolic Pathway	Gene symbol	log2Fold Change	lfcSE	p-value	padj
Lipid Metabolism					
Arachidonic acid metabolism	*PLA2G10*	2.967035	0.8093	0.00024	0.0238
	SLC27A2	2.242737	0.6604	0.00068	0.0402
	ALOXE3	2.499564	0.7524	0.00089	0.0456
Acylglycerides metabolism	*AADAC*	3.701064	0.9176	0.00005	0.0104
	MOGAT3	4.445076	1.1197	0.00007	0.0119
	MOGAT2	4.313961	1.0967	0.00008	0.0129
Glycerophospholipid metabolism	*PLA2G4F*	2.894178	0.7679	0.00016	0.0187
(Dysregulated)	*PLA2G10*	2.967035	0.8093	0.00024	0.0238
	CDS1	1.388428	0.3925	0.0004	0.0309
	GPCPD1	-0.96369	0.2875	0.0008	0.0443
Steroid metabolism	*FABP6*	4.422514	1.0898	0.00004	0.0102
	UGT1A1	5.423705	1.3737	0.00007	0.0124
	LIPA	-1.31671	0.3399	0.0001	0.0147
	SLCO1B3	5.378489	1.3883	0.0001	0.0147
	CYP3A4	4.066282	1.0721	0.00014	0.0177
	AKR1C4	3.64445	0.9716	0.00017	0.0196
	CETP	-2.29904	0.6137	0.00017	0.0199
	SLC27A2	2.242737	0.6604	0.00068	0.0402
	APOA4	7.120314	2.1282	0.00082	0.0447
	CLN8	-0.80028	0.2413	0.00091	0.0459

Bile acid biosynthesis and recycling	*SLCO1B3*	5.378489	1.3883	0.0001	0.0147
	CYP3A4	4.066282	1.0721	0.00014	0.0177
	AKR1C4	3.64445	0.9716	0.00017	0.0196
	SDR16C5	2.777176	0.8121	0.00062	0.0385
	SLC27A2	2.242737	0.6604	0.00068	0.0402
Ehter lipid metabolism	*PLA2G4F*	2.894178	0.7679	0.00016	0.0187
	PLA2G10	2.967035	0.8093	0.00024	0.0238
Glycosphingolipid metabolism	*B3GNT3*	2.636525	0.5695	0.000003	0.0023
	ALG1L	3.187208	0.7907	0.00005	0.0104
	FUT2	1.923234	0.5739	0.0008	0.0443
	UGT8	1.594161	0.4832	0.00096	0.0478
	ABO	2.275606	0.6935	0.00103	0.0492
Energy metabolism					
Oxydative phosphorylation	*ENTPD8*	3.229628	0.8303	0.0001	0.0143
Nitrogren metabolism	*CA9*	3.593014	1.0369	0.00053	0.0355
	CA13	1.457664	0.434	0.00078	0.0437
Carbohydrate metabolism					
Glycolysis / gluconeogenesis	*ALDH3A1*	3.900533	0.9499	0.00004	0.009
	HK3	-2.33905	0.6521	0.000335	0.02827
Tricarboxylic acid cycle and glyoxylate/dicarboxylate metabolism	*ALDH3A1*	3.900533	0.9499	0.00004	0.009
Fructose and mannose metabolism	*HK3*	-2.33905	0.6521	0.00033	0.0282
Ascorbate and aldarate metabolism	*UGT1A1*	5.423705	1.3737	0.00007	0.0124
Nucleotide metabolism	*NQO1*	2.306245	0.5791	0.00006	0.0117
	ENTPD8	3.229628	0.8304	0.0001	0.0143
	PDE2A	-1.94998	0.5045	0.00011	0.0149
	PDE7A	-1.37634	0.4019	0.00061	0.0384
Amino acid metabolism					
Alanine aspartate and glutamate metabolism	*GFPT1*	1.028761	0.3017	0.00065	0.0391
	IL4I1	-2.04549	0.6086	0.00077	0.0434
Glycine, serine and threonine metabolism	*CKMT1A*	2.587723	0.6042	0.00001	0.0054
	CKMT1B	2.533683	0.6274	0.00005	0.0103
Arginine and proline metabolism	*CKMT1A*	2.587723	0.6042	0.00001	0.0054
	CKMT1B	2.533683	0.6274	0.00005	0.0103
Histidine metabolism	*DDC*	3.974158	0.8558	0.00003	0.0023
	ALDH3A1	3.900533	0.9499	0.00004	0.009
	ELOVL6	1.335621	0.4073	0.00104	0.0492
Tyrosine metabolism	*DDC*	3.974158	0.8558	0.000003	0.0023
	ALDH3A1	3.900533	0.9499	0.00004	0.009
	IL4I1	-2.04549	0.6086	0.00077	0.0434
Amino sugar and nucleotide sugar metabolism					
(dysregulation)	NAGK	-0.77096	0.1904	0.000051	0.01028
	MANSC1	1.292456	0.3528	0.000249	0.02402
	HK3	-2.33904	0.6521	0.000334	0.02826
	CHI3L1	-2.62272	0.7549	0.000512	0.03467
	GFPT1	1.028760	0.3017	0.000650	0.03919
Cofactors and vitamins metabolism					
Porphyrin and chlorophyll metabolism	*HMOX1*	-1.88894	0.4378	0.00001	0.0051
	UGT1A1	5.423705	1.3737	0.00007	0.0124

Retinol metabolism	*AADAC*	3.701064	0.9176	0.00005	0.0104
	UGT1A1	5.423705	1.3737	0.00007	0.0124
	CYP3A4	4.066282	1.0721	0.00014	0.0177
	SDR16C5	2.777176	0.8121	0.00062	0.0385

Alternatively, the reporter metabolite algorithm (Patil and Nielsen, 2005) within the raven toolbox was used to uncover the metabolic alterations accompanied by the PDAC tumours. The algorithm benefits from the network topology provided by the reconstructed PDAC-specific GEM to recognise metabolic hotspots (Reporter Metabolites) associated with upregulated or downregulated genes in PDAC tumours. As a result, the algorithm detected 76 upregulated reporter metabolites and 35 downregulated reporter metabolites ($P<0.005$) regardless of their compartmentalisation.

Among the upregulated reporter metabolites were metabolites of the lipid metabolism such as arachidonic acid and its products like 19(S)-HETE, 16(R)-HETE, which takes part in the arachidonic acid metabolism. Also, the cytosolic acyl-CoA-LD-TG3 pool, fatty acid-LD-PC pool and fatty acid-LD-PE pool metabolites of the acyl glyceride metabolism were associated with upregulated genes. In the ether lipid metabolism, the O-1-alk-1-enyl-2-acyl-sn-glycero-3-phosphoethanolamine, 1-Organyl-2-lyso-sn-glycero-3-phosphocholine and 1-(1-alkenyl)-sn-glycero-3-phosphoethanolamine metabolites also demonstrated a significant association with upregulated genes. Reporter metabolites were also found in the amino acid metabolism as mitochondrial creatine and creatine-phosphate were also associated with upregulation of gene expression.

On the other hand, metabolites related to the carbohydrate metabolism showed association to gene expression downregulation. As an example, metabolites of the glycolysis and gluconeogenesis, which are beta D-glucose-6-phosphate and beta-D-glucose and metabolites of amino sugar and nucleotide sugar metabolism, and N-acetylglucosamine and N-acetylglucosamine-6-phosphate, respectively. Moreover, metabolites of the nucleotide metabolism showed different behaviour as the extracellular metabolites like UMP, IDP, IMP and UDP demonstrated an association to upregulated genes, while the metabolites like GMP, AMP,cyclic-AMP and cyclic-GMP showed their depletion in the nuclease and golgi apparatus.

Figure 3: Reporter metabolites results. Reporter metabolites with its associated subsystems in PDAC GEM for PDAC tumours n= 177 compared to noncancerous pancreas samples n=4. P-values for each reporter metabolite were calculated for up- and downregulated genes (student's t-test p-val <0.005), and the negative logarithm of the p-values are represented.

3.3 Implementation of DIRAC analysis and unsupervised clustering towards the stratification of PDAC patients

In order to find tightly regulated parts of the metabolism in PDAC, the DIRAC was used to analyse the normalised FPKM gene expression data using both of KEGG pathways and the PDAC-specific GEM subsystems. The population-level analysis was applied to find the rank conservation index for each network in the tumour phenotype which is a representative value for the degree of conservation in the rankings of the genes of the network expression value that is averaged over the phenotype samples. As a result, four pathways showed close levels of tight regulation in both of the used gene sets and those were oxidative phosphorylation, Cysteine and methionine metabolism, Beta-alanine metabolism and Riboflavin metabolism (table 2).

Table 2: Results from the DIRAC analysis. Four shared pathways between KEGG and PDAC GEM showed a close degree of tight regulation. The table shows the number of genes, gene pairs, average variance and the rank conservation index (mu_R) for each pathway across the used gene set collections.

	KEGG metabolic pathways				**PDAC GEM subsystems**			
pathway name	Num. genes	Num. pairs	Avg. variance	mu_R	Num. genes	Num. pairs	Avg. variance	mu_R
Oxidative phosphorylation	116	6670	2034.41	0.936	230	2633	1546.545	0.921
Cysteine and methionine metabolism	34	561	567.229	0.933	30	435	346.143	0.916
Beta alanine metabolism	22	231	433.489	0.932	11	55	660.701	0.875
Riboflavin metabolism	16	120	192.022	0.942	8	28	376.250	0.899

By extracting the four tightly regulated pathway gene content out of KEGG gene sets, a list of 152 unique genes was generated. Using the information about prognostic genes of pancreatic cancer from the pathology atlas of human cancer (Uhlen et al., 2017), the pathways genes were filtered based on their prognostic capability and out of the 152 genes, 14 genes were prognostic. Furthermore, using the top eight significantly prognostic genes in the consensus clustering of the 177 PDAC tumour samples applying the parameters mentioned in material and methods was accompanied by the best clustering consensus. The genes were: LDHA, ATP6VOD1, COX6B2, DNMT3A, UQCR11, ATP6VOA1, ATP6VOB and MTMR2. The analysis revealed that the best clustering of samples is into two groups, the first group (PDAC 1) consists of 88 patients and the second group (PDAC 2) consists of 89 patients with clustering consensus values 0.8774 and 0.8452 respectively (Appendix figure 1).

Next, survival analysis was performed on the two groups of the clustering analysis using clinical data of the 177 PDAC samples. The clinical data displayed information about the samples such as that the vital status of the patients was 85 alive and 92 dead until the last time the clinical data has been taken, and 21 samples were in the 1st stage, 146 in the 2nd stage, 3 in the 3rd stage, 4 in the 4th stage, while 3 were not reported. As a result, of the survival analysis, the p-value for the log-rank test between the two clusters was significant ($p\text{-val}<0.001$). The PDAC 1 group showed a significantly longer median survival time (913 days) in comparison to the PDAC 2 group (498 days) (figure 4A).

In order to gain more insight about the genetic alteration between the two cancer groups, differential expression analysis was performed using raw count data of the two groups as an input to the DEseq 2 R package. As a result, the analysis revealed that 1461 genes were expressed differentially (FDR adj. p-value < 0.05, log fold change cutoff > 1 or <-1). 330 of the DEGs were downregulated, and 1131 DEGs were upregulated based on their log fold change. By comparing those DEGs to the list of the prognostic genes from the pathology atlas, it was found that both data sets shared 139 genes. Finally, by looking into the differentially expressed genes within the list of eight genes used in the consensus clustering, six out of the eight were found to be DE, which included LDHA, ATP6VOD1, COX6B2, DNMT3A, ATP6VOA1, and MTMR2 (figure 4B).

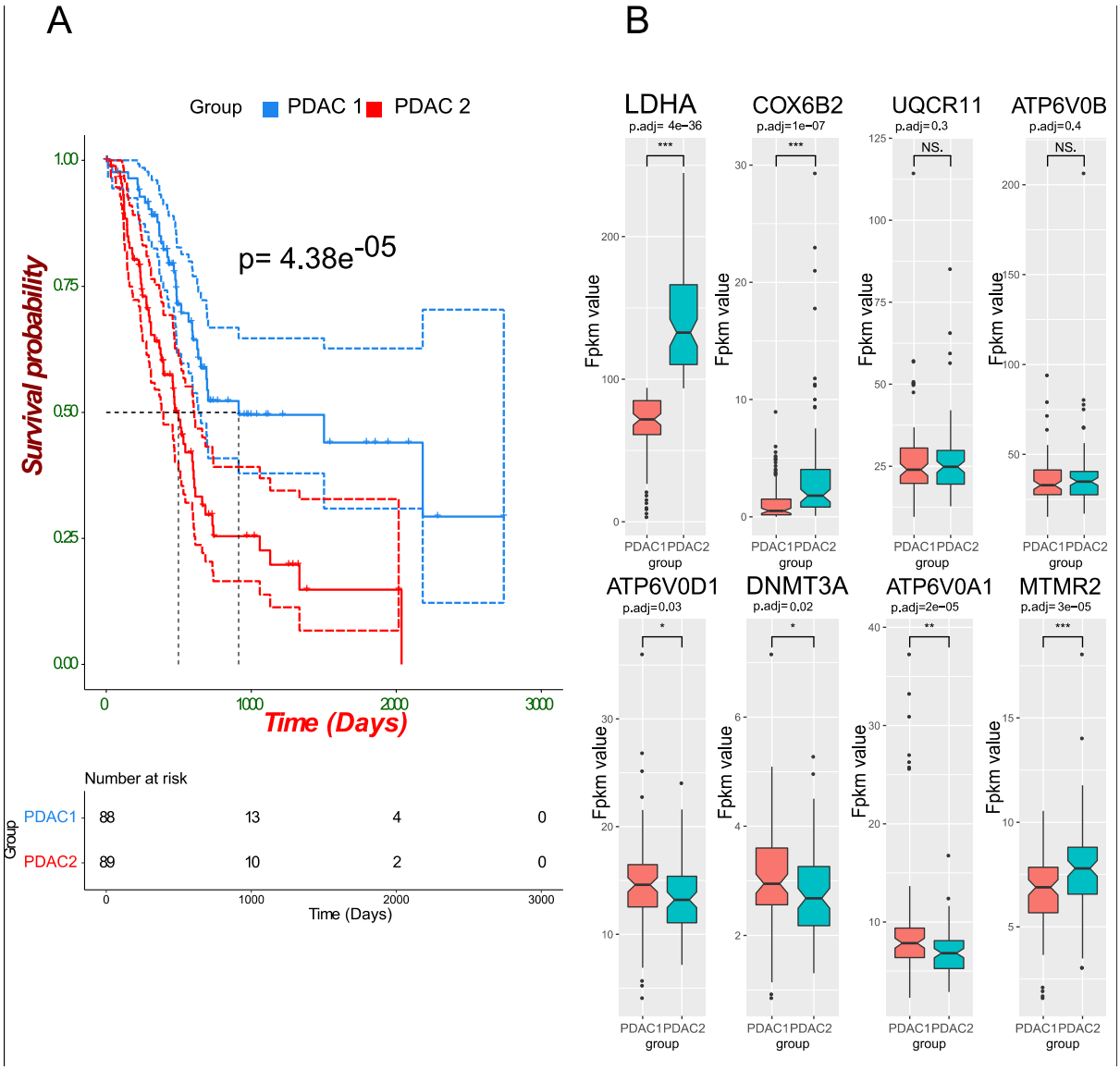

Figure 4: PDAC stratification analyses results. A) Overall survival analysis for the two PDAC groups resulted from the consensus clustering analysis. Kaplan-Meier plot showing the overall survival rate for patients of two cancer groups PDAC 1 (n=88) and PDAC 2 (N=89). The plot showed a significant difference in the median survival time (log-rank p-value=4.38^{e-05}) (solid line) with 95% confidence intervals (dashed lines for upper and lower bounds). B) Box plots for the distribution of FPKM values of the 8 genes used in the clustering analysis between the two PDAC groups n=88 and 89, respectively. Statistical significance determined by Wilcoxon test followed by FDR adjustment. * p<0.05.

Discussion

Genome-scale metabolic models are a mathematical representation of the current knowledge of metabolism where biochemical and physiological data on protein-encoding genes and their interactions with other bioactive compounds and associated reactions are integrated. These metabolic reconstructions were extensively used to study cancer metabolism and the underlying genetic alterations (Mardinoglu et al., 2018). The Availability of GEMs and its integration with a high-throughput omics data and methods of data analysis may enable increased understanding of the altered metabolism in cancer. In addition, the implementation of differential expression analysis, gene set analysis and differential rank conservation (DIRAC) analysis provides different information from gene expression data that can complement each other.

In line with the observed acylglycerides metabolism enrichment associated to the upregulation of Monoacylglycerol O-acyltransferase 2 and 3 (MOGAT2, MOGAT3) and Arylacetamide deacetylase (AADAC) in the pathway analysis (table1), the reporter metabolite results (figure 3) showed a significantly upregulated uptake of the cytosolic acyl-CoA-LD-TG3 pool and increased production of fatty acid-LD-PC pool and fatty acid-LD-PE pool. These are metabolites of the acylglecrides subsystem in the PDAC-specific reconstructed GEM. Both MOGAT2 and MOGAT3 genes are encoding for enzymes that catalyse the terminal step of the synthesis of triacylglycerol by using fatty acyl-CoA (cytosolic acyl-CoA-LD-TG3 pool) and diacylglycerol as substrates (Cheng et al., 2003, Brandt et al., 2016), which explains the increased uptake behaviour of the metabolite acyl-CoA-LD-TG3 pool (figure 3) in PDAC tumours. Moreover, the upregulated AADAC gene that encodes for a triacylglycerol lipase, an enzyme that catalyses the hydrolysis of the tri and diacylglycerols to increase the level of intracellular fatty acids (Nourbakhsh et al., 2013), suggests the reason behind the increased production levels of the fatty acid-LD-PC pool and fatty acid-LD-PE pool metabolites.

Another lipid metabolism-related pathway that was found to be associated with upregulated genes is the ether lipid metabolism (table1). The phospholipase A2 group X, Phospholipase A2 Group IVF (PLA2G4F, PLA2G10) are genes encoding for the enzyme phospholipase A2 that hydrolyse the glycerophospholipids in the sn-2 position and produce free fatty acids and lysophospholipids (Cupillard et al., 1997). Noticeably, this increase in the phospholipase A2 enzyme activity was clearly showing its effect at the metabolite level in the form of highly upregulated reporter metabolites that were associated with the ether lipid metabolism as shown in figure 3. Those reporter metabolites were O-1-alk-1-enyl-2-acyl-sn-glycero-3-phosphoethanolamine and 1-(1-alkenyl)-sn-glycero-3-phosphoethanolamine. These are the reactants that responded to the increased enzyme activity by increasing their levels and that lead to an increase in the fatty acid-LD-TG2 pool and 1-Organyl-2-lyso-sn-glycero-3-phosphocholine the products of the corresponding reactions. In a similar manner, the upregulated PLA2G10 demonstrated its powerful ability in the releasing of the arachidonic acid from the process of hydrolysing of phosphatidylcholine (Cupillard et al., 1997). That ability was shown by its relative increase in level from the results of the reporter metabolites along with other substrates of the metabolism of the arachidonic acid like 19(S)-HETE 16(R)-HETE were also found to be upregulated (figure 3).

Some of the analysed pathways did not show a clear association to upregulated or down genes, and those were considered as significantly dysregulated pathways within the gene set analysis. Amino sugar and nucleotide sugar metabolism, a part of the carbohydrate metabolism pathway, is an

example of the dysregulated pathways (table1), where genes like MANSC domain-containing protein 1 and Glutamine--fructose-6-phosphate aminotransferase [isomerising] 1 (MANSC1, GFPT1) were significantly upregulated. Contrarily, amino sugar and nucleotide sugar metabolism also had significantly downregulated genes. Among those genes was the N-acetyl-D-glucosamine kinase (NAGK) gene encoding the enzyme that degrades the N-acetylglucosamine to N-acetylglucosamine-6-phosphate (Bergfeld et al., 2012). Another gene was the Hexokinase-3 (HK3) glucose-phosphorylating isoenzyme that catalyses the phosphorylation of glucosamine to glucosamine-6-phosphate (Griffin et al., 1991). Also Chitinase-3-like protein 1 (CHI3L1) that encodes the enzyme which catalyses the hydrolysis of the β-1,4-N-acetyl-D-glucosamine linkages in chitin polymers and produces N-acetylglucosamine (Flach et al., 1992). This dysregulation was translated at the metabolite level by the decrease in the level of both N-acetylglucosamine and N-acetylglucosamine-6-phosphate in PDAC during the amino sugar and nucleotide sugar metabolism as presented by the reporter metabolite analysis (figure 3).

Glycolysis and Gluconeogenesis metabolism was one of the significantly altered pathways from the gene set analysis in PDAC that takes a part of the carbohydrate metabolism, and it showed an overall association to upregulated genes. Noticeably, only two genes were significantly differentially expressed in PDAC tumours as a result of the DE analysis, and they showed opposite levels of expression (table1). The first is aldehyde dehydrogenase 3 family member A1 (ALDH3A1), a gene that encodes for the aldehyde dehydrogenase [NAD(P)+] enzyme that catalyses the conversion between the acetate and acetaldehyde (Khanna et al., 2011), which was significantly upregulated in PDAC tumours. While the second gene is the previously mentioned Hexokinase-3 (HK3) glucose-phosphorylating isoenzyme and its role in this pathway is catalysing the phosphorylation of glucose to glucose-6-phosphate (Griffin et al., 1991). This gene was significantly downregulated in PDAC tumours. The significant downregulation of Hexokinase-3 can explain the appearance of both beta-D-glucose-6-phosphate and beta-D-glucose as a downregulated reporter metabolite. Noticeably, the upregulation of ALDH3A1 did not show a significant alteration on the metabolite level, which can partially be explained by it being affecting a peripheral reaction in this pathway.

A previous study of the altered metabolism of PDAC investigated the gene-metabolite interactions by utilising both transcriptomics and metabolomics to detect the tumour potential biomarkers and altered metabolic pathways (An et al., 2018). The study revealed pyrimidine metabolism as the most significant pathway and that Ectonucleoside Triphosphate diphosphohydrolase 8 (ENTPD8) is differentially downregulated in PDAC. ENTPD8 encodes the enzyme that catalyses the hydrolysis of gamma- and beta-phosphate residues of nucleotides, playing a central role in the concentration of extracellular nucleotides (Knowles and Li, 2006). Interestingly, in terms of pyrimidine metabolism significance and its association with ENTPD8, it matched the results of the GSA showed in our study. However, it did not match in terms of downregulation of the ENTPD8 (table1) as the DE analysis result here showed a significant upregulation of the gene. Notably, the survival analysis performed within the human pathology atlas study (Uhlen et al., 2017) based on the ENTPD8 expression showed a trend (not significant) towards that a shorter overall survival rate accompanies the increased gene expression. Concluding that the pathology atlas results supports the idea of overexpression of ENTPD8 is a pancreatic cancer trait, as shown in our study. In addition, the altered expression of the ENTPD8 can partially explain the accumulation of metabolites of the nucleotide metabolism like extracellular UMP, IDP, IMP and UDP and depletion in GMP, AMP,cyclic-AMP and cyclic-GMP in the nuclease and Golgi apparatus, that was demonstrated in the reporter metabolite analysis (figure2).

In order to detect PDAC metabolic networks that have significant alterations which maintain the cancer growth and spread, DIRAC analysis was performed. The algorithm can take into account the combinatorial differences in the tumour gene expression, which might have a critical impact on cellular behaviour. Briefly, for a specific gene set, the algorithm calculates the gene expression order and build a rank template based on the average ordering in each phenotype. Subsequently, it calculates the matching degree of each sample to the rank template that is termed the rank matching score and averaging this score across all samples yields the rank conservation index that measures the degree of entropy in a gene set. The network with low entropy is said to be tightly regulated while the one with high entropy is said to be loosely regulated (Eddy et al., 2010).

This algorithm has been used in several studies in order to find an underlying metabolic alteration in cancer. One study used the Dirac analysis and GEM reconstruction to find metabolic process required for the Hepatocellular carcinoma cell proliferation and showed a tight regulation of the fatty acid biosynthesis and deregulation of fatty acid oxidation (Bjornson et al., 2015). Another study applied the algorithm to study the metabolic alteration that is accompanied by prostate cancer. That study revealed significant metabolic alterations in the lipid metabolism including glycosphingolipid biosynthesis, ether lipid metabolism and steroid biosynthesis and pointed out changes in the metabolism of the pentose phosphate pathway as well as riboflavin metabolism (Turanli et al., 2019). In this project, the Algorithm used the network construction of the reconstructed PDAC-specific GEM in addition to the KEGG pathways and revealed the close results in the tight regulation of four metabolic pathways namely, oxidative phosphorylation, Cysteine and methionine metabolism, Beta-alanine metabolism and Riboflavin metabolism (table 2). Subsequently, the gene content of the four pathways was extracted and filtered based on its prognostic effect. Such information was derived from the results of the pathology atlas of the human cancer transcriptome, where the effect of the gene expression in the patient's survival rates was provided (Uhlen et al., 2017).

To find hidden patterns in the transcriptomics data that could be used for the PDAC stratification, the unsupervised class discovery has proven its efficacy in revealing PDAC groups that share common biological characteristics. The analysis was performed based on the top eight prognostic genes in the tightly regulated pathways as it detected two groups that showed genetic alterations between them (appendix figure 1). Moreover, to assess the results of the clustering, a survival analysis was performed using the clinical data for the 177 patients, which showed a significant difference in the survival outcome between the two groups of PDAC patients where the group PDAC1 had a significantly longer survival time compared to the PDAC2 group (figure 4A). Consequently, differential expression analysis was performed to detect the underlying genetic differences between the two PDAC groups. The analysis successfully detected 1461 genes that have possessed significantly altered expression with 1131 of them demonstrated an upregulated state while 330 were downregulated.

Interestingly, 139 of the differentially expressed genes between the PDAC groups were defined as prognostic genes in the pathology atlas. In addition, six out of the eight genes used in the classification process were differentially expressed, and they are LDHA, ATP6VOD1, COX6B2, DNMT3A, ATP6VOA1, and MTMR2. The L-lactate dehydrogenase A chain (LDHA*)* is a gene that encodes an enzyme that catalyses the reaction responsible for the production of the pyruvate and NADH from L-lactate and NAD (Adams et al., 1973). A previous study demonstrated the overexpression of the LDHA in pancreatic cancer and its ability to induce pancreatic cancer cell growth (Rong et al., 2013). In addition, knocking down the LDHA in the pancreatic cancer cells significantly inhibited the cell growth revealing

the oncogenic trait of LDHA and its association with poor prognosis (Rong et al., 2013). That was in parallel with the results introduced here where LDHA was significantly upregulated in the PDAC group with the poor survival rate. Another recent study evaluated the expression of LDHA by immunohistochemistry and correlated the results with clinicopathological characteristics and patient survival. Also, LDHA expression was assessed in 10 human pancreatic cancer cells and detected the significant overexpression of the gene and its association with the poor survival outcome (Mohammad et al., 2016). Those genes could be the basis for a potential gene signature that could be used for PDAC patients' stratification.

Conclusion and Future perspectives

In conclusion, this study has shed light on the undeniable value of using GEMs in deciphering the genetic and metabolic nature of cancer and overcome the heterogenic nature of some of the tumours. Here, the integration of both the transcriptomics and proteomics data represented a great added value as it allowed to include more information about PDAC and prevented potential false negatives that could be included during the GEM reconstruction. This significant value of integration was shown by the added 5244 genes from the TCGA data to the HPA data. The reconstructed PDAC specific GEM showed its ability to define metabolic alterations that were found in PDAC and provided consistent results with other gene sets like KEGG and GO biological processes during the GSA. The differentially expressed genes and reporter metabolites associated with the altered metabolic pathways in PDAC tumours including the lipid metabolism-related pathways (Ether lipid metabolism, Arachidonic acid metabolism, Acylglycerides metabolism) as well as carbohydrate metabolism (Ascorbate and aldarate metabolism, Glycolysis / Gluconeogenesis) in addition to Nucleotide metabolism are considered potential candidates as diagnostic biomarkers. Classification of the filtered DIRAC tightly regulated network genes based on their prognostic values from the pathology atlas managed to detect two groups of PDAC patients. The detected groups had a significantly different survival outcome, and the differential expression analysis showed that six of the eight genes used in clustering were showing significantly altered expression and suggesting their high value in PDAC patient stratification. One major wekanes of the study was the highly unbalanced data. For the future perspective, generating a more sufficient and balanced data is greatly desirable and with the fact that GEM is a great platform for data integration, starting to use more types of data is of great significance. Such data could be metabolomics that can provide a new aspect to the investigation, but it comes with the limitation that the prediction of the level of the metabolites intracellularly requires previous knowledge of thermodynamics and kinetics which is not clearly defined (Yizhak et al., 2010). Lastly, the systems-level analysis results allow for elucidating the undelaying altered metabolic mechanisms of PDAC that could provide more insights for the biomarker discovery and developing potential treatments.

Ethical aspects and impact of the research on society

The systems biology discipline is considered as a rapidly growing and interdisciplinary field (Westerhoff and Palsson, 2004). With the tremendous advances made by genomics and the massively produced high-throughput data, the role of systems biology comes to light for integrating this massive amount of data into a more comprehensive mathematical representation. Those mathematical models have more holistic predictions of the biological process that occurs in the living organisms. Due to the systems complex nature, the attempts to conceptualise the ethical, social and legal issues raised by systems biology faced a considerable proportion of complications. For that fact and despite its widespread practice, there has not been a concentration on the systems biology bioethical nor to its potential social consequences. The reason for the systems biology field to be exempt from the social and ethical considerations is mainly because of the vague nature of the questioned scientific object compared to other disciplines such as genomics. As one of the most attractive features of the systems biology approaches to the industry is the fact that it reduces experimental studies on living organisms and compensates that by the utilisation of the computer simulations (O'Malley et al., 2007). Such an attractive trait of the systems biology approach can be demonstrated in the in silico drug testing that can allow for exhaustive knowledge of side-effects and beneficial impact of drug usage before entering the clinical trial phase. Applying the systems biology approach plays a crucial rule in the cost reduction of the drug development process, which makes it attractive to the pharmaceutical companies. During the project, no ethical approval was needed. However, it is worth to notice that all the used datasets during *in silico* analysis were retrieved from public repositories where informed consents were obtained from patients who are involved in the research.

Acknowledgements

This work was financially supported by the Knut and Alice Wallenberg Foundation. I would like to express my gratitude and appreciation to my supervisor Adil Mardinoglu for his support and continuous guidance and to my colleagues Gholamreza Bidkhori, Muhammad Arif and Rui Benfeitas for sharing their knowledge and insights with me. My deepest gratefulness, appreciation and love goes to my family for supporting me by all manners throughout this journey. Thanks for believing in me.

References

Adams, M. J., Buehner, M., Chandrasekhar, K., Ford, G. C., Hackert, M. L., Liljas, A., Rossmann, M. G., Smiley, I. E., Allison, W. S., Everse, J., Kaplan, N. O. and Taylor, S. S. (1973) 'Structure-function relationships in lactate dehydrogenase', *Proc Natl Acad Sci U S A,* 70(7), pp. 1968-72.

Adamska, A., Domenichini, A. and Falasca, M. (2017) 'Pancreatic Ductal Adenocarcinoma: Current and Evolving Therapies', *Int J Mol Sci,* 18(7).

Agren, R., Bordel, S., Mardinoglu, A., Pornputtapong, N., Nookaew, I. and Nielsen, J. (2012) 'Reconstruction of genome-scale active metabolic networks for 69 human cell types and 16 cancer types using INIT', *PLoS Comput Biol,* 8(5), pp. e1002518.

Agren, R., Liu, L., Shoaie, S., Vongsangnak, W., Nookaew, I. and Nielsen, J. (2013) 'The RAVEN toolbox and its use for generating a genome-scale metabolic model for Penicillium chrysogenum', *PLoS Comput Biol,* 9(3), pp. e1002980.

Agren, R., Mardinoglu, A., Asplund, A., Kampf, C., Uhlen, M. and Nielsen, J. (2014) 'Identification of anticancer drugs for hepatocellular carcinoma through personalized genome-scale metabolic modeling', *Mol Syst Biol,* 10, pp. 721.

An, Y., Cai, H., Yang, Y., Zhang, Y., Liu, S., Wu, X., Duan, Y., Sun, D. and Chen, X. (2018) 'Identification of ENTPD8 and cytidine in pancreatic cancer by metabolomic and transcriptomic conjoint analysis', *Cancer Sci,* 109(9), pp. 2811-2821.

Bardeesy, N. and DePinho, R. A. (2002) 'Pancreatic cancer biology and genetics', *Nat Rev Cancer,* 2(12), pp. 897-909.

Bergfeld, A. K., Pearce, O. M., Diaz, S. L., Pham, T. and Varki, A. (2012) 'Metabolism of vertebrate amino sugars with N-glycolyl groups: elucidating the intracellular fate of the non-human sialic acid N-glycolylneuraminic acid', *J Biol Chem,* 287(34), pp. 28865-81.

Bjornson, E., Mukhopadhyay, B., Asplund, A., Pristovsek, N., Cinar, R., Romeo, S., Uhlen, M., Kunos, G., Nielsen, J. and Mardinoglu, A. (2015) 'Stratification of Hepatocellular Carcinoma Patients Based on Acetate Utilization', *Cell Rep,* 13(9), pp. 2014-26.

Bordbar, A. and Palsson, B. O. (2012) 'Using the reconstructed genome-scale human metabolic network to study physiology and pathology', *J Intern Med,* 271(2), pp. 131-41.

Brandt, C., McFie, P. J. and Stone, S. J. (2016) 'Biochemical characterization of human acyl coenzyme A: 2-monoacylglycerol acyltransferase-3 (MGAT3)', *Biochem Biophys Res Commun,* 475(3), pp. 264-70.

Cairns, R. A. and Mak, T. W. (2016) 'The current state of cancer metabolism FOREWORD', *Nat Rev Cancer,* 16(10), pp. 613-614.

Cheng, D., Nelson, T. C., Chen, J., Walker, S. G., Wardwell-Swanson, J., Meegalla, R., Taub, R., Billheimer, J. T., Ramaker, M. and Feder, J. N. (2003) 'Identification of acyl coenzyme A:monoacylglycerol acyltransferase 3, an intestinal specific enzyme implicated in dietary fat absorption', *J Biol Chem,* 278(16), pp. 13611-4.

Croft, D., O'Kelly, G., Wu, G., Haw, R., Gillespie, M., Matthews, L., Caudy, M., Garapati, P., Gopinath, G., Jassal, B., Jupe, S., Kalatskaya, I., Mahajan, S., May, B., Ndegwa, N., Schmidt, E., Shamovsky, V., Yung, C., Birney, E., Hermjakob, H., D'Eustachio, P. and Stein, L. (2011) 'Reactome: a database of reactions, pathways and biological processes', *Nucleic Acids Res,* 39(Database issue), pp. D691-7.

Cupillard, L., Koumanov, K., Mattei, M. G., Lazdunski, M. and Lambeau, G. (1997) 'Cloning, chromosomal mapping, and expression of a novel human secretory phospholipase A2', *J Biol Chem,* 272(25), pp. 15745-52.

DeBerardinis, R. J. and Chandel, N. S. (2016) 'Fundamentals of cancer metabolism', *Sci Adv,* 2(5), pp. e1600200.

DeBerardinis, R. J. and Thompson, C. B. (2012) 'Cellular metabolism and disease: what do metabolic outliers teach us?', *Cell,* 148(6), pp. 1132-44.

Duarte, N. C., Becker, S. A., Jamshidi, N., Thiele, I., Mo, M. L., Vo, T. D., Srivas, R. and Palsson, B. O. (2007) 'Global reconstruction of the human metabolic network based on genomic and bibliomic data', *Proc Natl Acad Sci U S A,* 104(6), pp. 1777-82.

Eddy, J. A., Hood, L., Price, N. D. and Geman, D. (2010) 'Identifying tightly regulated and variably expressed networks by Differential Rank Conservation (DIRAC)', *PLoS Comput Biol,* 6(5), pp. e1000792.

Fagerberg, L., Hallstrom, B. M., Oksvold, P., Kampf, C., Djureinovic, D., Odeberg, J., Habuka, M., Tahmasebpoor, S., Danielsson, A., Edlund, K., Asplund, A., Sjostedt, E., Lundberg, E., Szigyarto, C. A., Skogs, M., Takanen, J. O., Berling, H., Tegel, H., Mulder, J., Nilsson, P., Schwenk, J. M., Lindskog, C., Danielsson, F., Mardinoglu, A., Sivertsson, A., von Feilitzen, K., Forsberg, M., Zwahlen, M., Olsson, I., Navani, S., Huss, M., Nielsen, J., Ponten, F. and Uhlen, M. (2014) 'Analysis of the human tissue-specific expression by genome-wide integration of transcriptomics and antibody-based proteomics', *Mol Cell Proteomics,* 13(2), pp. 397-406.

Ferlay, J., Soerjomataram, I., Dikshit, R., Eser, S., Mathers, C., Rebelo, M., Parkin, D. M., Forman, D. and Bray, F. (2015) 'Cancer incidence and mortality worldwide: sources, methods and major patterns in GLOBOCAN 2012', *Int J Cancer,* 136(5), pp. E359-86.

Flach, J., Pilet, P. E. and Jolles, P. (1992) 'What's new in chitinase research?', *Experientia,* 48(8), pp. 701-16.

Fondi, M. and Lio, P. (2015) 'Genome-scale metabolic network reconstruction', *Methods Mol Biol,* 1231, pp. 233-56.

Ghaffari, P., Mardinoglu, A. and Nielsen, J. (2015) 'Cancer Metabolism: A Modeling Perspective', *Front Physiol,* 6, pp. 382.

Gille, C., Bolling, C., Hoppe, A., Bulik, S., Hoffmann, S., Hubner, K., Karlstadt, A., Ganeshan, R., Konig, M., Rother, K., Weidlich, M., Behre, J. and Holzhutter, H. G. (2010) 'HepatoNet1: a comprehensive metabolic reconstruction of the human hepatocyte for the analysis of liver physiology', *Mol Syst Biol,* 6, pp. 411.

Greaves, M. and Maley, C. C. (2012) 'Clonal evolution in cancer', *Nature,* 481(7381), pp. 306-13.

Griffin, L. D., Gelb, B. D., Wheeler, D. A., Davison, D., Adams, V. and McCabe, E. R. (1991) 'Mammalian hexokinase 1: evolutionary conservation and structure to function analysis', *Genomics,* 11(4), pp. 1014-24.

Grossman, R. L., Heath, A. P., Ferretti, V., Varmus, H. E., Lowy, D. R., Kibbe, W. A. and Staudt, L. M. (2016) 'Toward a Shared Vision for Cancer Genomic Data', *N Engl J Med,* 375(12), pp. 1109-12.

Hanahan, D. and Weinberg, R. A. (2000) 'The hallmarks of cancer', *Cell,* 100(1), pp. 57-70.

Hanahan, D. and Weinberg, R. A. (2011) 'Hallmarks of cancer: the next generation', *Cell,* 144(5), pp. 646-74.

Kanehisa, M. and Goto, S. (2000) 'KEGG: kyoto encyclopedia of genes and genomes', *Nucleic Acids Res,* 28(1), pp. 27-30.

Khanna, M., Chen, C. H., Kimble-Hill, A., Parajuli, B., Perez-Miller, S., Baskaran, S., Kim, J., Dria, K., Vasiliou, V., Mochly-Rosen, D. and Hurley, T. D. (2011) 'Discovery of a novel class of covalent inhibitor for aldehyde dehydrogenases', *J Biol Chem,* 286(50), pp. 43486-94.

Knowles, A. F. and Li, C. (2006) 'Molecular cloning and characterization of expressed human ecto-nucleoside triphosphate diphosphohydrolase 8 (E-NTPDase 8) and its soluble extracellular domain', *Biochemistry,* 45(23), pp. 7323-33.

Lazar, M. A. and Birnbaum, M. J. (2012) 'Physiology. De-meaning of metabolism', *Science,* 336(6089), pp. 1651-2.

Le, A., Cooper, C. R., Gouw, A. M., Dinavahi, R., Maitra, A., Deck, L. M., Royer, R. E., Vander Jagt, D. L., Semenza, G. L. and Dang, C. V. (2010) 'Inhibition of lactate dehydrogenase A induces oxidative stress and inhibits tumor progression', *Proc Natl Acad Sci U S A,* 107(5), pp. 2037-42.

Lewis, N. E., Nagarajan, H. and Palsson, B. O. (2012) 'Constraining the metabolic genotype-phenotype relationship using a phylogeny of in silico methods', *Nat Rev Microbiol,* 10(4), pp. 291-305.

Liang, C., Qin, Y., Zhang, B., Ji, S., Shi, S., Xu, W., Liu, J., Xiang, J., Liang, D., Hu, Q., Ni, Q., Xu, J. and Yu, X. (2016) 'Metabolic plasticity in heterogeneous pancreatic ductal adenocarcinoma', *Biochim Biophys Acta,* 1866(2), pp. 177-188.

Liberzon, A., Birger, C., Thorvaldsdottir, H., Ghandi, M., Mesirov, J. P. and Tamayo, P. (2015) 'The Molecular Signatures Database (MSigDB) hallmark gene set collection', *Cell Syst,* 1(6), pp. 417-425.

Lohr, M., Kloppel, G., Maisonneuve, P., Lowenfels, A. B. and Luttges, J. (2005) 'Frequency of K-ras mutations in pancreatic intraductal neoplasias associated with pancreatic ductal adenocarcinoma and chronic pancreatitis: a meta-analysis', *Neoplasia,* 7(1), pp. 17-23.

Love, M. I., Huber, W. and Anders, S. (2014) 'Moderated estimation of fold change and dispersion for RNA-seq data with DESeq2', *Genome Biol,* 15(12), pp. 550.

Ma, H., Sorokin, A., Mazein, A., Selkov, A., Selkov, E., Demin, O. and Goryanin, I. (2007) 'The Edinburgh human metabolic network reconstruction and its functional analysis', *Mol Syst Biol,* 3, pp. 135.

Mardinoglu, A., Boren, J., Smith, U., Uhlen, M. and Nielsen, J. (2018) 'Systems biology in hepatology: approaches and applications', *Nat Rev Gastroenterol Hepatol,* 15(6), pp. 365-377.

Mardinoglu, A., Gatto, F. and Nielsen, J. (2013) 'Genome-scale modeling of human metabolism - a systems biology approach', *Biotechnol J,* 8(9), pp. 985-96.

Mardinoglu, A. and Nielsen, J. (2012) 'Systems medicine and metabolic modelling', *J Intern Med,* 271(2), pp. 142-54.

Mardinoglu, A. and Nielsen, J. (2015) 'New paradigms for metabolic modeling of human cells', *Curr Opin Biotechnol,* 34, pp. 91-7.

McKnight, S. L. (2010) 'On getting there from here', *Science,* 330(6009), pp. 1338-9.

Mohammad, G. H., Olde Damink, S. W., Malago, M., Dhar, D. K. and Pereira, S. P. (2016) 'Pyruvate Kinase M2 and Lactate Dehydrogenase A Are Overexpressed in Pancreatic Cancer and Correlate with Poor Outcome', *PLoS One,* 11(3), pp. e0151635.

Nilsson, A. and Nielsen, J. (2017) 'Genome scale metabolic modeling of cancer', *Metab Eng,* 43(Pt B), pp. 103-112.

Nourbakhsh, M., Douglas, D. N., Pu, C. H., Lewis, J. T., Kawahara, T., Lisboa, L. F., Wei, E., Asthana, S., Quiroga, A. D., Law, L. M., Chen, C., Addison, W. R., Nelson, R., Houghton, M., Lehner, R. and Kneteman, N. M. (2013) 'Arylacetamide deacetylase: a novel host factor with important roles in the lipolysis of cellular triacylglycerol stores, VLDL assembly and HCV production', *J Hepatol,* 59(2), pp. 336-43.

O'Malley, M. A., Calvert, J. and Dupre, J. (2007) 'The study of socioethical issues in systems biology', *Am J Bioeth,* 7(4), pp. 67-78.

Orth, J. D., Thiele, I. and Palsson, B. O. (2010) 'What is flux balance analysis?', *Nat Biotechnol,* 28(3), pp. 245-8.

Patil, K. R. and Nielsen, J. (2005) 'Uncovering transcriptional regulation of metabolism by using metabolic network topology', *Proc Natl Acad Sci U S A,* 102(8), pp. 2685-9.

Pavlova, N. N. and Thompson, C. B. (2016) 'The Emerging Hallmarks of Cancer Metabolism', *Cell Metab,* 23(1), pp. 27-47.

Perera, R. M. and Bardeesy, N. (2015) 'Pancreatic Cancer Metabolism: Breaking It Down to Build It Back Up', *Cancer Discov,* 5(12), pp. 1247-61.

Price, N. D., Reed, J. L. and Palsson, B. O. (2004) 'Genome-scale models of microbial cells: evaluating the consequences of constraints', *Nat Rev Microbiol,* 2(11), pp. 886-97.

Rahib, L., Smith, B. D., Aizenberg, R., Rosenzweig, A. B., Fleshman, J. M. and Matrisian, L. M. (2014) 'Projecting cancer incidence and deaths to 2030: the unexpected burden of thyroid, liver, and pancreas cancers in the United States', *Cancer Res,* 74(11), pp. 2913-21.

Romero, P., Wagg, J., Green, M. L., Kaiser, D., Krummenacker, M. and Karp, P. D. (2005) 'Computational prediction of human metabolic pathways from the complete human genome', *Genome Biol,* 6(1), pp. R2.

Rong, Y., Wu, W., Ni, X., Kuang, T., Jin, D., Wang, D. and Lou, W. (2013) 'Lactate dehydrogenase A is overexpressed in pancreatic cancer and promotes the growth of pancreatic cancer cells', *Tumour Biol,* 34(3), pp. 1523-30.

Schmidt, B. J., Papin, J. A. and Musante, C. J. (2013) 'Mechanistic systems modeling to guide drug discovery and development', *Drug Discov Today,* 18(3-4), pp. 116-27.

Siegel, R. L., Miller, K. D. and Jemal, A. (2016) 'Cancer statistics, 2016', *CA Cancer J Clin,* 66(1), pp. 7-30.

Son, J., Lyssiotis, C. A., Ying, H., Wang, X., Hua, S., Ligorio, M., Perera, R. M., Ferrone, C. R., Mullarky, E., Shyh-Chang, N., Kang, Y., Fleming, J. B., Bardeesy, N., Asara, J. M., Haigis, M. C., DePinho,

R. A., Cantley, L. C. and Kimmelman, A. C. (2013) 'Glutamine supports pancreatic cancer growth through a KRAS-regulated metabolic pathway', *Nature,* 496(7443), pp. 101-5.

Sousa, C. M. and Kimmelman, A. C. (2014) 'The complex landscape of pancreatic cancer metabolism', *Carcinogenesis,* 35(7), pp. 1441-50.

Sud, M., Fahy, E., Cotter, D., Brown, A., Dennis, E. A., Glass, C. K., Merrill, A. H., Jr., Murphy, R. C., Raetz, C. R., Russell, D. W. and Subramaniam, S. (2007) 'LMSD: LIPID MAPS structure database', *Nucleic Acids Res,* 35(Database issue), pp. D527-32.

Therneau, T. M. and Lumley, T. (2018) 'Package 'survival''.

Thiele, I. and Palsson, B. O. (2010) 'A protocol for generating a high-quality genome-scale metabolic reconstruction', *Nat Protoc,* 5(1), pp. 93-121.

Tian, Q., Price, N. D. and Hood, L. (2012) 'Systems cancer medicine: towards realization of predictive, preventive, personalized and participatory (P4) medicine', *J Intern Med,* 271(2), pp. 111-21.

Turanli, B., Zhang, C., Kim, W., Benfeitas, R., Uhlen, M., Arga, K. Y. and Mardinoglu, A. (2019) 'Discovery of therapeutic agents for prostate cancer using genome-scale metabolic modeling and drug repositioning', *EBioMedicine,* 42, pp. 386-396.

Uhlén, M., Fagerberg, L., Hallström, B. M., Lindskog, C., Oksvold, P., Mardinoglu, A., Sivertsson, Å., Kampf, C., Sjöstedt, E., Asplund, A., Olsson, I., Edlund, K., Lundberg, E., Navani, S., Szigyarto, C. A.-K., Odeberg, J., Djureinovic, D., Takanen, J. O., Hober, S., Alm, T., Edqvist, P.-H., Berling, H., Tegel, H., Mulder, J., Rockberg, J., Nilsson, P., Schwenk, J. M., Hamsten, M., von Feilitzen, K., Forsberg, M., Persson, L., Johansson, F., Zwahlen, M., von Heijne, G., Nielsen, J. and Pontén, F. (2015) 'Tissue-based map of the human proteome', *Science,* 347.

Uhlen, M., Zhang, C., Lee, S., Sjostedt, E., Fagerberg, L., Bidkhori, G., Benfeitas, R., Arif, M., Liu, Z., Edfors, F., Sanli, K., von Feilitzen, K., Oksvold, P., Lundberg, E., Hober, S., Nilsson, P., Mattsson, J., Schwenk, J. M., Brunnstrom, H., Glimelius, B., Sjoblom, T., Edqvist, P. H., Djureinovic, D., Micke, P., Lindskog, C., Mardinoglu, A. and Ponten, F. (2017) 'A pathology atlas of the human cancer transcriptome', *Science,* 357(6352).

Varemo, L., Nielsen, J. and Nookaew, I. (2013) 'Enriching the gene set analysis of genome-wide data by incorporating directionality of gene expression and combining statistical hypotheses and methods', *Nucleic Acids Res,* 41(8), pp. 4378-91.

Varemo, L., Scheele, C., Broholm, C., Mardinoglu, A., Kampf, C., Asplund, A., Nookaew, I., Uhlen, M., Pedersen, B. K. and Nielsen, J. (2015) 'Proteome- and transcriptome-driven reconstruction of the human myocyte metabolic network and its use for identification of markers for diabetes', *Cell Rep,* 11(6), pp. 921-933.

Vincent, A., Herman, J., Schulick, R., Hruban, R. H. and Goggins, M. (2011) 'Pancreatic cancer', *Lancet,* 378(9791), pp. 607-20.

Warburg, O. (1956) 'On the origin of cancer cells', *Science,* 123(3191), pp. 309-14.

Warburg, O., Wind, F. and Negelein, E. (1927) 'The Metabolism of Tumors in the Body', *J Gen Physiol,* 8(6), pp. 519-30.

Weinhouse, S. (1951) 'Studies on the fate of isotopically labeled metabolites in the oxidative metabolism of tumors', *Cancer Res,* 11(8), pp. 585-91.

Weinhouse, S. (1956) 'On respiratory impairment in cancer cells', *Science,* 124(3215), pp. 267-9.

Weinhouse, S. (1972) 'Glycolysis, respiration, and anomalous gene expression in experimental hepatomas: G.H.A. Clowes memorial lecture', *Cancer Res,* 32(10), pp. 2007-16.

Westerhoff, H. V. and Palsson, B. O. (2004) 'The evolution of molecular biology into systems biology', *Nat Biotechnol,* 22(10), pp. 1249-52.

Wilkerson, M. D. and Hayes, D. N. (2010) 'ConsensusClusterPlus: a class discovery tool with confidence assessments and item tracking', *Bioinformatics,* 26(12), pp. 1572-3.

Ying, H., Kimmelman, A. C., Lyssiotis, C. A., Hua, S., Chu, G. C., Fletcher-Sananikone, E., Locasale, J. W., Son, J., Zhang, H., Coloff, J. L., Yan, H., Wang, W., Chen, S., Viale, A., Zheng, H., Paik, J. H., Lim, C., Guimaraes, A. R., Martin, E. S., Chang, J., Hezel, A. F., Perry, S. R., Hu, J., Gan, B., Xiao, Y., Asara, J. M., Weissleder, R., Wang, Y. A., Chin, L., Cantley, L. C. and DePinho, R. A. (2012) 'Oncogenic Kras maintains pancreatic tumors through regulation of anabolic glucose metabolism', *Cell,* 149(3), pp. 656-70.

Yizhak, K., Benyamini, T., Liebermeister, W., Ruppin, E. and Shlomi, T. (2010) 'Integrating quantitative proteomics and metabolomics with a genome-scale metabolic network model', *Bioinformatics,* 26(12), pp. i255-60.

Yizhak, K., Chaneton, B., Gottlieb, E. and Ruppin, E. (2015) 'Modeling cancer metabolism on a genome scale', *Mol Syst Biol,* 11(6), pp. 817.

Appendix

Table Appendix 1: the connectivity genes in the PDAC specific GEM. Details on the 38 genes incorporated to PDAC-specific GEM for enhancing the model connectivity. Each gene is shown in the context of its associated reaction and subsystem in the PDAC-specific GEM.

connectivity genes	REACTION ID in HMR2	REACTION EQUATION	SUBSYSTEM
ENSG00000185818	HMR_8626	acetyl-CoA[m] + aspartate[m] => CoA[m] + N-acetyl-L-aspartate[m]	Alanine, aspartate and glutamate metabolism
ENSG00000122787	HMR_2014	4-androstene-3,17-dione[c] + H+[c] + NADPH[c] => 5alpha-androstane-3,17-dione[c] + NADP+[c]	Androgen metabolism
ENSG00000172508	HMR_4606	4-aminobutyrate[c] + ATP[c] + histidine[c] => AMP[c] + homocarnosine[c] + PPi[c]	Arginine and proline metabolism
ENSG00000242110	HMR_3491	(2R)-pristanoyl-CoA[p] <=> (2S)-pristanoyl-CoA[p]	Beta oxidation of phytanic acid (peroxisomal)
ENSG00000105398	HMR_1729	chenodiol[c] + H+[c] + PAPS[c] => PAP[c] + sulfochenodeoxycholate[c]	Bile acid biosynthesis
ENSG00000146233	HMR_1737	24-hydroxycholesterol[c] + H+[c] + NADPH[c] + O2[c] => cholest-5-ene-3beta,7alpha,24(S)-triol[c] + H2O[c] + NADP+[c]	Bile acid biosynthesis
ENSG00000167910	HMR_1581	cholesterol[r] + H+[r] + NADPH[r] + O2[r] => 7alpha-hydroxycholesterol[r] + H2O[r] + NADP+[r]	Bile acid biosynthesis
ENSG00000180432	HMR_1590	7alpha-hydroxycholest-4-en-3-one[r] + H+[r] + NADH[r] + O2[r] => 7alpha,12alpha-dihydroxycholest-4-en-3-one[r] + H2O[r] + NAD+[r]	Bile acid biosynthesis
ENSG00000198610	HMR_1742	5beta-cholestan-7alpha,12alpha,24(S)-triol-3-one[c] + H+[c] + NADPH[c] => 5beta-cholestan-3alpha,7alpha,12alpha,24(S)-tetrol[c] + NADP+[c]	Bile acid biosynthesis
ENSG00000111700	HMR_1881	cholate[s] + HCO3-[c] + S-glutathionyl-2-4-dinitrobenzene[c] <=> cholate[c] + HCO3-[s] + S-glutathionyl-2-4-dinitrobenzene[s]	Bile acid recycling
ENSG00000160200	HMR_3879	homocysteine[c] + serine[c] => H2O[c] + L-cystathionine[c]	Cysteine and methionine metabolism
ENSG00000160868	HMR_2046	estradiol-17beta[c] + H+[c] + NADPH[c] + O2[c] => 4-hydroxy-17beta-estradiol[c] + H2O[c] + NADP+[c]	Estrogen metabolism
ENSG00000116882	HMR_7703	glycolate[c] + O2[c] => glyoxalate[c] + H2O2[c]	Glycine, serine and threonine metabolism
ENSG00000124713	HMR_3901	glycine[c] + SAM[c] => SAH[c] + sarcosine[c]	Glycine, serine and threonine metabolism
ENSG00000172482	HMR_4198	pyruvate[m] + serine[m] => alanine[m] + hydroxypyruvate[m]	Glycine, serine and threonine metabolism
ENSG00000172461	HMR_0893	GDP-L-fucose[c] + nLc8Cer[c] => G00084[c] + GDP[c]	Glycosphingolipid biosynthesis-lacto and neolacto series
ENSG00000256062	HMR_0867	IV2Fuc-Lc4Cer[c] + UDP-N-acetyl-D-galactosamine[c] => type I A glycolipid[c] + UDP[c]	Glycosphingolipid biosynthesis-lacto and neolacto series

ENSG00000184886	HMR_7187	6-(alpha-D-glucosaminyl)-1-phosphatidyl-1D-myo-inositol[r] + palmitoyl-CoA[r] => CoA[r] + glucosaminyl-acylphosphatidylinositol[r]	Glycosylphosphatidylinositol (GPI)-anchor biosynthesis
ENSG00000127080	HMR_6576	1D-myo-inositol-1,3,4,5,6-pentakisphosphate[c] + ATP[c] => ADP[c] + myo-inositol-hexakisphosphate[c]	Inositol phosphate metabolism
ENSG00000182621	HMR_8818	H2O[n] + phosphatidylinositol-4,5-bisphosphate[n] => 1,2-diacylglycerol-LD-TAG pool[n] + D-myo-inositol-1,4,5-trisphosphate[n]	Inositol phosphate metabolism
ENSG00000213316	HMR_1081	GSH[c] + leukotriene A4[c] => leukotriene C4[c]	Leukotriene metabolism
ENSG00000130649	HMR_7099	1,2-dibromoethane[c] + H+[c] + NADPH[c] + O2[c] => 2-bromoacetaldehyde[c] + H2O[c] + hydrobromic acid[c] + NADP+[c]	Metabolism of xenobiotics by cytochrome P450
ENSG00000140505	HMR_7018	aflatoxin B1[c] + H+[c] + NADPH[c] + O2[c] => aflatoxin M1[c] + H2O[c] + NADP+[c]	Metabolism of xenobiotics by cytochrome P450
ENSG00000198488	HMR_7174	Tn-antigen[g] + UDP-N-acetylglucosamine[g] => core 3[g] + UDP[g]	O-glycan metabolism
ENSG00000132330	HMR_7133	alanine[c] + pyridoxal-phosphate[c] + selenide[c] <=> pyridoxine-phosphate[c] + selenocysteine[c]	Other amino acid
ENSG00000077498	HMR_6874	O2[c] + tyrosine[c] => H2O[c] + L-dopaquinone[c]	Phenylalanine, tyrosine and tryptophan biosynthesis
ENSG00000117009	HMR_4220	H+[c] + kynurenine[c] + NADPH[c] + O2[c] => 3-hydroxy-L-kynurenine[c] + H2O[c] + NADP+[c]	Phenylalanine, tyrosine and tryptophan biosynthesis
ENSG00000121053	HMR_6813	dopaminochrome[c] + 2 H+[c] + H2O[c] <=> dopamine-O-quinone[c] + H2O2[c]	Phenylalanine, tyrosine and tryptophan biosynthesis
ENSG00000158104	HMR_6772	4-hydroxyphenylpyruvate[c] + O2[c] => CO2[c] + homogentisate[c]	Phenylalanine, tyrosine and tryptophan biosynthesis
ENSG00000129673	HMR_4546	acetyl-CoA[c] + serotonin[c] => CoA[c] + N-acetyl-serotonin[c]	Serotonin and melatonin biosynthesis
ENSG00000196433	HMR_4547	N-acetyl-serotonin[c] + SAM[c] => melatonin[c] + SAH[c]	Serotonin and melatonin biosynthesis
ENSG00000135454	HMR_8165	LacCer pool[g] + UDP-N-acetyl-D-galactosamine[g] => GA2[g] + UDP[g]	Sphingolipid metabolism
ENSG00000140459	HMR_7935	cholesterol[m] + H+[m] + NADPH[m] + 2 O2[m] => 2 H2O[m] + isocaproic-aldehyde[m] + NADP+[m] + pregnenolone[m]	Steroid metabolism
ENSG00000203859	HMR_7930	NAD+[c] + pregnenolone[c] => H+[c] + NADH[c] + progesterone[c]	Steroid metabolism
ENSG00000081800	HMR_7904	Na+[s] + selenate[s] => Na+[c] + selenate[c]	Transport, extracellular
ENSG00000084453	HMR_6060	GSH[c] + HCO3-[c] + lithocholate[s] <=> GSH[s] + HCO3-[s] + lithocholate[c]	Transport, extracellular
ENSG00000132677	HMR_4873	NH3[c] <=> NH3[s]	Transport, extracellular
ENSG00000134538	HMR_6107	bilirubin-monoglucuronoside[s] + GSH[c] + HCO3-[c] <=> bilirubin-monoglucuronoside[c] + GSH[s] + HCO3-[s]	Transport, extracellular

Table Appendix 2: PDAC tumour vs matched normal tissues DE analysis results. The complete list of differentially expressed genes (FDR adj. p-value < 0.05, LFC cutoff >1or<-1) between PDAC tumours (n=177) and noncancerous Pancreas tissue(n=4) is provided. The significance level of differential expression sorts the genes: upregulated gene highlighted (green) and downregulated genes highlighted (red).

Ensembl gene id	gene name	baseMean	log2FoldChange	lfcSE	stat	pvalue	padj
ENSG00000090402	SI	141.345332	23.78471401	2.11199	11.26176	2.03E-29	5.27E-25
ENSG00000110245	APOC3	67.62635	22.13061296	2.164321	10.2252	1.53E-24	1.99E-20
ENSG00000164816	DEFA5	21.4507779	20.90206495	3.111877	6.716867	1.86E-11	1.61E-07
ENSG00000204019	CT83	37.0038532	16.96919279	2.618592	6.480274	9.16E-11	5.95E-07
ENSG00000248115	AC023154.1	5.94421651	-4.485669972	0.703321	-6.37784	1.80E-10	8.75E-07
ENSG00000233024	AC126755.2	3.29691156	-3.270036661	0.514163	-6.35993	2.02E-10	8.75E-07
ENSG00000223668	EEF1A1P24	14.0243833	-3.025561254	0.511938	-5.91002	3.42E-09	1.27E-05
ENSG00000136011	STAB2	92.1522949	-4.670613423	0.81512	-5.72997	1.00E-08	3.26E-05
ENSG00000188375	H3F3C	14.7585402	-2.302268954	0.404053	-5.69794	1.21E-08	3.50E-05
ENSG00000232656	IDI2-AS1	5.44854512	-3.343407724	0.589465	-5.67194	1.41E-08	3.67E-05
ENSG00000167653	PSCA	10524.9959	6.527410466	1.171677	5.570999	2.53E-08	5.99E-05
ENSG00000150045	KLRF1	34.4699128	-2.977961453	0.549679	-5.41764	6.04E-08	0.000131
ENSG00000043355	ZIC2	62.6822428	7.784236227	1.485449	5.240324	1.60E-07	0.000321
ENSG00000156886	ITGAD	32.7992677	-3.786719143	0.740467	-5.11396	3.15E-07	0.000513
ENSG00000168356	SCN11A	23.3097779	-3.052050802	0.5941	-5.13726	2.79E-07	0.000513
ENSG00000279166	AC009951.1	3.1877019	-2.646569926	0.517525	-5.11389	3.16E-07	0.000513
ENSG00000272620	AFAP1-AS1	1796.26017	4.706809422	0.926917	5.077919	3.82E-07	0.000584
ENSG00000163283	ALPP	147.250515	7.61589268	1.508226	5.049569	4.43E-07	0.00064
ENSG00000237757	EEF1A1P30	5.71103293	-1.785992117	0.355126	-5.02918	4.93E-07	0.000674
ENSG00000144452	ABCA12	190.506458	3.968519508	0.790979	5.017222	5.24E-07	0.000681
ENSG00000137441	FGFBP2	23.3114674	-3.032674188	0.605756	-5.00643	5.54E-07	0.000686
ENSG00000166143	PPP1R14D	352.463377	4.076930371	0.817742	4.985595	6.18E-07	0.00073
ENSG00000130720	FIBCD1	479.081173	5.150278379	1.041302	4.946	7.58E-07	0.000856
ENSG00000134539	KLRD1	159.585863	-2.804644666	0.570519	-4.91595	8.84E-07	0.000957
ENSG00000274414	AL121772.1	67.7250691	3.290597025	0.679527	4.842483	1.28E-06	0.001334
ENSG00000262406	MMP12	987.051742	-3.947561842	0.819322	-4.81809	1.45E-06	0.001415
ENSG00000120907	ADRA1A	10.7737345	-3.499902786	0.731996	-4.78131	1.74E-06	0.001415
ENSG00000124664	SPDEF	1616.11804	4.002164654	0.834495	4.795913	1.62E-06	0.001415
ENSG00000179066	AC020907.1	42.4139843	4.695685884	0.980444	4.789345	1.67E-06	0.001415
ENSG00000117983	MUC5B	18483.8027	4.901324538	1.024129	4.785847	1.70E-06	0.001415
ENSG00000187908	DMBT1	12329.8325	5.254564648	1.091355	4.814717	1.47E-06	0.001415
ENSG00000114248	LRRC31	208.91411	5.315928562	1.107096	4.801687	1.57E-06	0.001415
ENSG00000143869	GDF7	120.850722	-3.154337737	0.662072	-4.76434	1.89E-06	0.001493
ENSG00000261123	AC009065.5	184.534128	3.130674935	0.665795	4.702162	2.57E-06	0.001968
ENSG00000173702	MUC13	10613.7685	3.661190535	0.785335	4.661949	3.13E-06	0.002262
ENSG00000166535	A2ML1	480.922337	6.337481049	1.358428	4.665304	3.08E-06	0.002262
ENSG00000226239	AL031658.1	7.84220364	-2.59639942	0.561347	-4.6253	3.74E-06	0.002372
ENSG00000179913	B3GNT3	5039.07448	2.636525103	0.569543	4.629192	3.67E-06	0.002372
ENSG00000089356	FXYD3	15639.807	3.025428617	0.653442	4.629988	3.66E-06	0.002372
ENSG00000132437	DDC	527.009795	3.974157781	0.85582	4.643682	3.42E-06	0.002372
ENSG00000198788	MUC2	880.374935	7.49819315	1.620295	4.627673	3.70E-06	0.002372
ENSG00000225411	CR786580.1	3.02109358	-3.015185976	0.65504	-4.60306	4.16E-06	0.002577
ENSG00000117472	TSPAN1	14204.5641	2.851790076	0.623609	4.573042	4.81E-06	0.00284
ENSG00000173557	C2orf70	189.943985	3.266425838	0.713643	4.577114	4.71E-06	0.00284
ENSG00000163286	ALPPL2	102.449133	6.426869896	1.411355	4.553687	5.27E-06	0.003046
ENSG00000161640	SIGLEC11	52.8677664	-3.1914933	0.701739	-4.54798	5.42E-06	0.003061
ENSG00000073861	TBX21	63.1456333	-2.817946451	0.624743	-4.51057	6.47E-06	0.003502
ENSG00000241560	ZBTB20-AS1	4.6488207	-2.426332827	0.537665	-4.51272	6.40E-06	0.003502
ENSG00000163687	DNASE1L3	110.211053	-3.810258276	0.851043	-4.47716	7.56E-06	0.003594
ENSG00000261644	AC007728.2	14.0494759	-2.593900382	0.581884	-4.45776	8.28E-06	0.003594
ENSG00000281103	TRG-AS1	74.2589396	-2.563085132	0.574825	-4.4589	8.24E-06	0.003594
ENSG00000168010	ATG16L2	1233.66923	-1.721209253	0.383635	-4.48658	7.24E-06	0.003594
ENSG00000104081	BMF	1397.96055	-1.517088945	0.33994	-4.46281	8.09E-06	0.003594
ENSG00000060140	STYK1	568.879499	2.698522371	0.605399	4.457431	8.29E-06	0.003594
ENSG00000151012	SLC7A11	870.646737	2.865690535	0.637561	4.494772	6.96E-06	0.003594
ENSG00000203697	CAPN8	6864.3862	3.594674858	0.803667	4.47284	7.72E-06	0.003594
ENSG00000134398	ERN2	4487.21877	3.795176065	0.843606	4.498756	6.84E-06	0.003594

ENSG00000224511	LINC00365	46.876301	3.821710493	0.852292	4.484037	7.32E-06	0.003594
ENSG00000137440	FGFBP1	573.583081	4.505188902	1.010685	4.457558	8.29E-06	0.003594
ENSG00000167656	LY6D	1834.48987	6.244928285	1.39536	4.475495	7.62E-06	0.003594
ENSG00000104974	LILRA1	54.9944618	-2.528761528	0.568462	-4.44843	8.65E-06	0.003687
ENSG00000242797	GLYCTK-AS1	7.52415936	-2.279388232	0.513846	-4.43594	9.17E-06	0.003788
ENSG00000180251	SLC9A4	229.528154	5.754514238	1.297337	4.435637	9.18E-06	0.003788
ENSG00000231483	AL365356.4	21.3270335	4.177177669	0.94678	4.411985	1.02E-05	0.004161
ENSG00000157368	IL34	327.991253	-1.946747665	0.441887	-4.40553	1.06E-05	0.004169
ENSG00000074211	PPP2R2C	723.361174	3.807549996	0.864387	4.404914	1.06E-05	0.004169
ENSG00000169247	SH3TC2	183.248237	2.643710736	0.601279	4.396812	1.10E-05	0.004263
ENSG00000143768	LEFTY2	20.0178496	-2.963590626	0.674639	-4.39285	1.12E-05	0.004277
ENSG00000267432	DNAH17-AS1	11.1359669	-3.414411644	0.78098	-4.37196	1.23E-05	0.004574
ENSG00000111679	PTPN6	3240.77592	-1.338651213	0.306148	-4.37256	1.23E-05	0.004574
ENSG00000135723	FHOD1	1494.18231	-1.086342508	0.24877	-4.36686	1.26E-05	0.004616
ENSG00000168229	PTGDR	44.4262708	-2.383962063	0.546389	-4.36312	1.28E-05	0.00463
ENSG00000242136	AC093904.2	10.2039418	5.882498465	1.349461	4.359147	1.31E-05	0.00465
ENSG00000172478	C2orf54	565.166382	3.01825455	0.693313	4.353379	1.34E-05	0.00471
ENSG00000264345	LINC01894	2.8886384	-3.545013692	0.816673	-4.3408	1.42E-05	0.004879
ENSG00000104369	JPH1	402.616228	2.517973309	0.580206	4.339789	1.43E-05	0.004879
ENSG00000259933	AC009065.2	202.471089	2.890996472	0.666656	4.336567	1.45E-05	0.004887
ENSG00000076356	PLXNA2	4102.81231	1.556734514	0.359902	4.325441	1.52E-05	0.00501
ENSG00000164237	CMBL	2526.50731	1.878494589	0.434107	4.327259	1.51E-05	0.00501
ENSG00000188993	LRRC66	435.363947	3.346997249	0.774853	4.319527	1.56E-05	0.005082
ENSG00000100292	HMOX1	1836.03229	-1.88894292	0.437854	-4.31409	1.60E-05	0.005144
ENSG00000279277	AC012020.1	12.5002665	-2.037484312	0.472844	-4.309	1.64E-05	0.0052
ENSG00000257207	AC112229.3	32.4988241	-2.168500068	0.503835	-4.30399	1.68E-05	0.005215
ENSG00000169684	CHRNA5	222.102281	2.465808472	0.57304	4.303028	1.68E-05	0.005215
ENSG00000165828	PRAP1	590.486487	4.852541776	1.130666	4.291757	1.77E-05	0.005359
ENSG00000249395	CASC9	97.3730375	7.032465879	1.637792	4.293871	1.76E-05	0.005359
ENSG00000223572	CKMT1A	315.261322	2.587722621	0.60429	4.282254	1.85E-05	0.005466
ENSG00000261857	MIA	704.146645	4.156903379	0.970401	4.283696	1.84E-05	0.005466
ENSG00000180745	CLRN3	580.425345	3.681416126	0.860236	4.279543	1.87E-05	0.005471
ENSG00000146094	DOK3	598.456549	-1.988011107	0.465352	-4.27206	1.94E-05	0.005595
ENSG00000129226	CD68	112.641419	-1.986556347	0.467929	-4.24542	2.18E-05	0.006166
ENSG00000158373	HIST1H2BD	736.99528	2.419690661	0.570662	4.240148	2.23E-05	0.006245
ENSG00000182957	SPATA13	2106.01316	-1.005060973	0.237963	-4.2236	2.40E-05	0.00665
ENSG00000117009	KMO	104.464246	-2.265222599	0.536702	-4.22064	2.44E-05	0.006667
ENSG00000146192	FGD2	763.792602	-2.099754908	0.497909	-4.21715	2.47E-05	0.006701
ENSG00000161798	AQP5	3625.03478	4.129864841	0.980887	4.210336	2.55E-05	0.006835
ENSG00000133328	HRASLS2	240.935462	3.811522641	0.906221	4.205953	2.60E-05	0.006869
ENSG00000168631	DPCR1	14579.8744	5.239457277	1.246129	4.204585	2.62E-05	0.006869
ENSG00000180818	HOXC10	232.605163	5.467228174	1.302695	4.196858	2.71E-05	0.007036
ENSG00000137251	TINAG	92.5880233	4.711004519	1.125603	4.185315	2.85E-05	0.007259
ENSG00000248290	TNXA	9.20758171	-3.054045862	0.737888	-4.1389	3.49E-05	0.007959
ENSG00000184293	CLECL1	44.4202899	-2.967861303	0.714907	-4.1514	3.30E-05	0.007959
ENSG00000181036	FCRL6	51.7559835	-2.673890175	0.645552	-4.14202	3.44E-05	0.007959
ENSG00000126838	PZP	11.5588575	-2.235180079	0.537826	-4.15595	3.24E-05	0.007959
ENSG00000187808	SOWAHD	67.7182908	-1.906217533	0.460451	-4.13989	3.47E-05	0.007959
ENSG00000228486	LINC01125	85.1103515	-1.645330136	0.396587	-4.14872	3.34E-05	0.007959
ENSG00000180596	HIST1H2BC	167.249934	2.667238876	0.641955	4.154866	3.25E-05	0.007959
ENSG00000128298	BAIAP2L2	2246.88028	2.876571362	0.693666	4.146909	3.37E-05	0.007959
ENSG00000265763	ZNF488	185.642332	3.114559985	0.752284	4.140141	3.47E-05	0.007959
ENSG00000103355	PRSS33	103.39512	4.879325984	1.174667	4.153793	3.27E-05	0.007959
ENSG00000259439	LINC01833	78.6434202	5.253640528	1.266911	4.146811	3.37E-05	0.007959
ENSG00000163295	ALPI	34.3053844	6.915729493	1.662547	4.159719	3.19E-05	0.007959
ENSG00000000938	FGR	895.758467	-2.092645908	0.508675	-4.11392	3.89E-05	0.008795
ENSG00000108602	ALDH3A1	849.53075	3.900533448	0.949919	4.106173	4.02E-05	0.009016
ENSG00000180644	PRF1	394.645047	-2.085147275	0.51024	-4.0866	4.38E-05	0.009727
ENSG00000182580	EPHB3	1856.08509	2.350324761	0.575458	4.084268	4.42E-05	0.009742
ENSG00000253988	AC079015.1	3.83641219	-2.873850335	0.704132	-4.08141	4.48E-05	0.00978
ENSG00000234750	AC012618.2	6.80765972	-2.101909178	0.515267	-4.07926	4.52E-05	0.009788
ENSG00000184678	HIST2H2BE	1456.46891	2.213924543	0.543791	4.071278	4.68E-05	0.010046
ENSG00000227467	LINC01537	16.4058457	-2.535227066	0.625173	-4.05524	5.01E-05	0.010284

ENSG00000237484	LINC01684	9.51490348	-2.523586183	0.622705	-4.05262	5.06E-05	0.010284
ENSG00000008516	MMP25	131.716028	-1.788640432	0.441092	-4.05503	5.01E-05	0.010284
ENSG00000103460	TOX3	1014.22833	2.262441731	0.558464	4.051184	5.10E-05	0.010284
ENSG00000088836	SLC4A11	962.689374	2.587780324	0.639074	4.049268	5.14E-05	0.010284
ENSG00000181378	CFAP65	86.7202328	3.457421405	0.852879	4.053825	5.04E-05	0.010284
ENSG00000170231	FABP6	139.661567	4.422513922	1.089825	4.058002	4.95E-05	0.010284
ENSG00000163586	FABP1	138.201088	6.136367016	1.512116	4.058132	4.95E-05	0.010284
ENSG00000203499	IQANK1	888.950174	2.2445397	0.554979	4.04437	5.25E-05	0.010286
ENSG00000278912	AC008870.5	61.3578295	3.928511162	0.9712	4.045008	5.23E-05	0.010286
ENSG00000244280	ECEL1P2	37.1443897	4.887715489	1.208731	4.043674	5.26E-05	0.010286
ENSG00000141232	TOB1	5280.88171	1.534596967	0.379854	4.039961	5.35E-05	0.010372
ENSG00000237289	CKMT1B	389.916197	2.533683314	0.627466	4.037964	5.39E-05	0.010384
ENSG00000172738	TMEM217	56.3864847	-1.976253521	0.490701	-4.02741	5.64E-05	0.010481
ENSG00000166947	EPB42	8.78417289	-1.810668913	0.449606	-4.02724	5.64E-05	0.010481
ENSG00000246228	CASC8	133.944913	3.179954207	0.789562	4.027489	5.64E-05	0.010481
ENSG00000189366	ALG1L	119.448401	3.187208212	0.790741	4.030662	5.56E-05	0.010481
ENSG00000114771	AADAC	508.738667	3.701064382	0.91767	4.033109	5.50E-05	0.010481
ENSG00000135750	KCNK1	3020.15427	2.072060576	0.514833	4.02472	5.70E-05	0.010518
ENSG00000269220	LINC00528	29.9174742	-2.42252816	0.60356	-4.01373	5.98E-05	0.010872
ENSG00000254759	NAP1L1P1	17.2225061	-1.183797899	0.294946	-4.01361	5.98E-05	0.010872
ENSG00000261583	AC012317.1	13.7603795	5.599952717	1.397923	4.00591	6.18E-05	0.011154
ENSG00000270919	AC108451.2	14.0480994	5.619606928	1.403791	4.003164	6.25E-05	0.011207
ENSG00000175311	ANKS4B	647.226072	3.145249216	0.787206	3.995458	6.46E-05	0.011498
ENSG00000179546	HTR1D	308.874858	2.738626995	0.686537	3.989048	6.63E-05	0.011654
ENSG00000101188	NTSR1	584.031283	4.577159136	1.147357	3.989308	6.63E-05	0.011654
ENSG00000126759	CFP	213.313811	-2.560393896	0.642266	-3.9865	6.71E-05	0.0117
ENSG00000255819	KLRC4-KLRK1	7.02125418	-2.790550781	0.701546	-3.97771	6.96E-05	0.011792
ENSG00000136379	ABHD17C	3747.00138	2.188561321	0.549924	3.979754	6.90E-05	0.011792
ENSG00000181019	NQO1	11060.3302	2.306244956	0.579129	3.982265	6.83E-05	0.011792
ENSG00000111291	GPRC5D	68.2054583	2.627424194	0.660687	3.976804	6.98E-05	0.011792
ENSG00000183128	CALHM3	195.957727	4.434633439	1.114364	3.97952	6.91E-05	0.011792
ENSG00000115648	MLPH	9572.45931	2.226595362	0.560419	3.973089	7.09E-05	0.011866
ENSG00000159263	SIM2	457.823733	2.662002348	0.670152	3.972237	7.12E-05	0.011866
ENSG00000106384	MOGAT3	75.7620167	4.445075748	1.119759	3.969673	7.20E-05	0.011918
ENSG00000178789	CD300LB	83.3587539	-2.196047586	0.554199	-3.96256	7.42E-05	0.012202
ENSG00000160606	TLCD1	464.689713	1.687093137	0.42601	3.960215	7.49E-05	0.012244
ENSG00000135218	CD36	1613.71898	-2.871027057	0.725603	-3.95675	7.60E-05	0.012256
ENSG00000138964	PARVG	988.403024	-2.115214485	0.53445	-3.95774	7.57E-05	0.012256
ENSG00000152689	RASGRP3	827.882121	-1.438525828	0.363676	-3.95552	7.64E-05	0.012256
ENSG00000166839	ANKDD1A	281.156119	-1.172978374	0.29694	-3.95021	7.81E-05	0.012454
ENSG00000241635	UGT1A1	53.5976523	5.423704953	1.373728	3.948165	7.88E-05	0.012485
ENSG00000272789	AC010976.2	25.9839271	-2.523698606	0.639455	-3.94664	7.93E-05	0.012488
ENSG00000158717	RNF166	968.791202	-1.19469148	0.30298	-3.94314	8.04E-05	0.012596
ENSG00000262319	AC007952.6	2.9663061	-3.562839822	0.907557	-3.92575	8.65E-05	0.012991
ENSG00000140955	ADAD2	10.7540728	-2.559485831	0.651925	-3.92604	8.64E-05	0.012991
ENSG00000105374	NKG7	306.654941	-2.259943845	0.575611	-3.92617	8.63E-05	0.012991
ENSG00000104972	LILRB1	349.601957	-2.181667745	0.554973	-3.93112	8.45E-05	0.012991
ENSG00000177202	SPACA4	59.561175	3.098283756	0.788384	3.929916	8.50E-05	0.012991
ENSG00000137860	SLC28A2	76.458182	4.296826661	1.093172	3.930603	8.47E-05	0.012991
ENSG00000166391	MOGAT2	171.942415	4.313960552	1.096754	3.933388	8.38E-05	0.012991
ENSG00000124102	PI3	1711.70421	3.703489245	0.944618	3.920622	8.83E-05	0.013121
ENSG00000007264	MATK	201.276974	-2.047253232	0.522636	-3.91717	8.96E-05	0.013235
ENSG00000178462	TUBAL3	22.8436988	4.520108337	1.156107	3.909766	9.24E-05	0.01357
ENSG00000109255	NMU	444.162353	3.541490933	0.906162	3.908231	9.30E-05	0.01358
ENSG00000161929	SCIMP	323.379616	-2.392541087	0.613742	-3.89829	9.69E-05	0.014071
ENSG00000121210	TMEM131L	1007.79122	-1.807849321	0.464275	-3.89392	9.86E-05	0.014169
ENSG00000163501	IHH	763.147275	3.587048893	0.920912	3.895104	9.82E-05	0.014169
ENSG00000133710	SPINK5	467.779739	3.178739845	0.817416	3.888765	0.000101	0.014314
ENSG00000188833	ENTPD8	574.064419	3.229628018	0.830397	3.889256	0.000101	0.014314
ENSG00000235505	AP002004.1	158.597697	-1.763899206	0.454571	-3.88036	0.000104	0.014501
ENSG00000115616	SLC9A2	478.314471	3.42637424	0.882873	3.880937	0.000104	0.014501
ENSG00000166869	CHP2	68.7835382	6.286909036	1.619219	3.88268	0.000103	0.014501
ENSG00000107798	LIPA	5077.46457	-1.316706992	0.339986	-3.87283	0.000108	0.014721

ENSG00000111700	SLCO1B3	102.19161	5.37848897	1.388354	3.874005	0.000107	0.014721
ENSG00000163219	ARHGAP25	799.566121	-2.006030531	0.518896	-3.86596	0.000111	0.014967
ENSG00000186642	PDE2A	562.661659	-1.949976116	0.504526	-3.86497	0.000111	0.014967
ENSG00000261104	AC093904.4	31.150678	4.002221082	1.03547	3.865124	0.000111	0.014967
ENSG00000179583	CIITA	1914.56773	-1.970386892	0.510214	-3.86188	0.000113	0.015037
ENSG00000178597	PSAPL1	256.359416	5.529507198	1.432027	3.861314	0.000113	0.015037
ENSG00000220412	AL356234.1	9.75702107	-2.658644326	0.689236	-3.85738	0.000115	0.015126
ENSG00000173868	PHOSPHO1	37.9924854	-1.944861098	0.504121	-3.85792	0.000114	0.015126
ENSG00000167851	CD300A	774.145799	-1.66217883	0.431324	-3.85367	0.000116	0.015279
ENSG00000174837	ADGRE1	54.0257489	-2.28133016	0.59573	-3.82947	0.000128	0.016643
ENSG00000158555	GDPD5	989.674316	-1.377526921	0.359659	-3.83009	0.000128	0.016643
ENSG00000179292	TMEM151A	204.131952	3.370204665	0.88046	3.827778	0.000129	0.016643
ENSG00000248996	AC145098.1	22.189718	-1.980254519	0.517914	-3.82352	0.000132	0.016768
ENSG00000196420	S100A5	36.5992671	2.331618709	0.609811	3.823509	0.000132	0.016768
ENSG00000204613	TRIM10	99.4383646	2.680715718	0.701435	3.821759	0.000133	0.016805
ENSG00000105523	FAM83E	2490.47547	2.561435547	0.67111	3.816712	0.000135	0.017069
ENSG00000151715	TMEM45B	2385.18774	2.388951024	0.626164	3.815219	0.000136	0.017089
ENSG00000227039	ITGB2-AS1	265.816891	-2.55213807	0.671081	-3.80302	0.000143	0.017352
ENSG00000251322	SHANK3	1451.96982	-1.397013076	0.367436	-3.80206	0.000143	0.017352
ENSG00000168453	HR	933.524147	2.178521822	0.572683	3.804064	0.000142	0.017352
ENSG00000183856	IQGAP3	1338.19046	2.293170701	0.602946	3.803276	0.000143	0.017352
ENSG00000119946	CNNM1	406.205496	2.4017631	0.630804	3.807462	0.00014	0.017352
ENSG00000166126	AMN	1506.80111	3.036079123	0.797926	3.804964	0.000142	0.017352
ENSG00000253293	HOXA10	235.560755	3.58902979	0.943715	3.803087	0.000143	0.017352
ENSG00000204614	TRIM40	14.3479982	5.657868956	1.486179	3.806989	0.000141	0.017352
ENSG00000138162	TACC2	2786.27533	1.429319912	0.376893	3.792381	0.000149	0.01773
ENSG00000280032	AP002800.1	70.9325281	3.008896263	0.793454	3.79215	0.000149	0.01773
ENSG00000189280	GJB5	390.588077	3.581476954	0.944304	3.792717	0.000149	0.01773
ENSG00000160868	CYP3A4	69.2575522	4.066281712	1.072147	3.792651	0.000149	0.01773
ENSG00000122223	CD244	60.2049644	-2.148700119	0.567173	-3.78844	0.000152	0.017754
ENSG00000107551	RASSF4	2509.705	-1.5389546	0.406121	-3.7894	0.000151	0.017754
ENSG00000108798	ABI3	748.426276	-1.500577419	0.395989	-3.78944	0.000151	0.017754
ENSG00000238057	ZEB2-AS1	11.8352676	-1.686583706	0.445569	-3.78524	0.000154	0.017808
ENSG00000196754	S100A2	3791.51385	4.433680375	1.171365	3.785054	0.000154	0.017808
ENSG00000215182	MUC5AC	20702.1678	4.51563206	1.193449	3.783682	0.000155	0.017808
ENSG00000242207	HOXB-AS4	23.6040924	4.994398215	1.320137	3.783242	0.000155	0.017808
ENSG00000028277	POU2F2	484.774945	-2.237780056	0.592397	-3.7775	0.000158	0.018143
ENSG00000168907	PLA2G4F	199.953157	2.894177583	0.767936	3.768774	0.000164	0.018707
ENSG00000115607	IL18RAP	76.716891	-2.17355608	0.57711	-3.76627	0.000166	0.018813
ENSG00000240143	AL023653.1	6.5464776	-2.616176823	0.695223	-3.76307	0.000168	0.018876
ENSG00000143850	PLEKHA6	5442.55153	1.492077514	0.396599	3.762186	0.000168	0.018876
ENSG00000106789	CORO2A	3161.04782	1.932277883	0.513464	3.763219	0.000168	0.018876
ENSG00000198610	AKR1C4	66.6444885	3.644450291	0.971663	3.750736	0.000176	0.019674
ENSG00000087237	CETP	106.642614	-2.299043225	0.613729	-3.74602	0.00018	0.019961
ENSG00000228952	LINC02041	51.6929628	2.846782166	0.760197	3.744797	0.000181	0.019974
ENSG00000267731	AC005332.5	20.2406114	-2.222643261	0.594425	-3.73915	0.000185	0.020086
ENSG00000197943	PLCG2	1561.49068	-1.646647617	0.440306	-3.73978	0.000184	0.020086
ENSG00000099812	MISP	7174.10653	2.258671087	0.604017	3.739414	0.000184	0.020086
ENSG00000104827	CGB3	19.4195724	6.815745029	1.822683	3.739403	0.000184	0.020086
ENSG00000230882	AC005077.4	145.831081	2.866146027	0.767893	3.732483	0.00019	0.020539
ENSG00000185332	TMEM105	119.025344	2.621034786	0.702851	3.729149	0.000192	0.020641
ENSG00000257588	AC025154.2	153.721227	3.256621143	0.873069	3.730085	0.000191	0.020641
ENSG00000100055	CYTH4	910.476704	-1.725355068	0.462975	-3.72667	0.000194	0.020759
ENSG00000122133	PAEP	123.192067	4.460033946	1.198623	3.720963	0.000198	0.021147
ENSG00000130812	ANGPTL6	33.0553968	-1.957941853	0.526572	-3.71828	0.000201	0.021286
ENSG00000221968	FADS3	1042.66125	-1.27303874	0.34274	-3.7143	0.000204	0.021448
ENSG00000238133	MAP3K20-AS1	196.234463	4.058350875	1.092453	3.714898	0.000203	0.021448
ENSG00000245694	CRNDE	355.863147	2.141504368	0.577303	3.709497	0.000208	0.021771
ENSG00000137101	CD72	478.580024	-2.227100881	0.601066	-3.70525	0.000211	0.021926
ENSG00000160182	TFF1	21199.7615	4.236032239	1.14336	3.704899	0.000211	0.021926
ENSG00000016490	CLCA1	314.325873	6.860356477	1.851819	3.704658	0.000212	0.021926
ENSG00000211829	TRDC	42.5110414	-2.204799525	0.595789	-3.70064	0.000215	0.022013
ENSG00000140968	IRF8	1923.85756	-2.091315754	0.565017	-3.70133	0.000214	0.022013

ENSG00000166959	MS4A8	919.335402	3.409001217	0.92071	3.70258	0.000213	0.022013
ENSG00000114346	ECT2	1674.01072	1.658690489	0.448534	3.698024	0.000217	0.022154
ENSG00000053747	LAMA3	12756.447	2.344485106	0.634856	3.692939	0.000222	0.022513
ENSG00000213809	KLRK1	24.6990727	-2.536704812	0.688397	-3.68495	0.000229	0.02304
ENSG00000251323	AP003086.1	6.79595243	-2.144046551	0.58213	-3.68311	0.00023	0.02304
ENSG00000157214	STEAP2	2242.97579	1.330181552	0.361109	3.683605	0.00023	0.02304
ENSG00000145681	HAPLN1	105.633947	3.47405567	0.942669	3.68534	0.000228	0.02304
ENSG00000211689	TRGC1	24.6578434	-2.483456459	0.675448	-3.67675	0.000236	0.023088
ENSG00000254760	AC008750.1	5.84544257	-2.23556026	0.607839	-3.67788	0.000235	0.023088
ENSG00000229029	CDCA4P1	3.91596056	-2.159983701	0.586948	-3.68003	0.000233	0.023088
ENSG00000093100	AC016026.1	7.54942003	-1.798142757	0.488805	-3.67865	0.000234	0.023088
ENSG00000065413	ANKRD44	825.679707	-1.718191211	0.467305	-3.67681	0.000236	0.023088
ENSG00000170545	SMAGP	1599.69568	1.642656196	0.446546	3.678582	0.000235	0.023088
ENSG00000235111	Z97192.3	5.82804264	-2.4653049	0.671544	-3.6711	0.000242	0.023517
ENSG00000234883	MIR155HG	71.9359182	-1.990005688	0.542433	-3.66867	0.000244	0.023653
ENSG00000069764	PLA2G10	258.545215	2.967034647	0.809345	3.665972	0.000246	0.023815
ENSG00000105609	LILRB5	228.381969	-2.456839915	0.671284	-3.65991	0.000252	0.024028
ENSG00000117245	KIF17	95.7717088	-1.770880703	0.483697	-3.66113	0.000251	0.024028
ENSG00000111261	MANSC1	2731.95269	1.292456118	0.352877	3.662625	0.00025	0.024028
ENSG00000103269	RHBDL1	180.753124	2.342191945	0.639928	3.660084	0.000252	0.024028
ENSG00000233532	LINC00460	104.377823	3.567854408	0.975143	3.6588	0.000253	0.024044
ENSG00000164236	ANKRD33B	200.60836	-1.99045327	0.544913	-3.65279	0.000259	0.024425
ENSG00000145416	1-Mar	623.538807	-1.737296058	0.475714	-3.65197	0.00026	0.024425
ENSG00000162545	CAMK2N1	7328.62319	1.429770029	0.391483	3.652193	0.00026	0.024425
ENSG00000173467	AGR3	1990.63261	2.997125171	0.821325	3.649133	0.000263	0.024608
ENSG00000064270	ATP2C2	1080.25131	2.229371635	0.611996	3.642789	0.00027	0.025132
ENSG00000142347	MYO1F	1444.00639	-1.63170336	0.448266	-3.64004	0.000273	0.025312
ENSG00000237928	NFIA-AS2	22.0255813	-2.398770222	0.659717	-3.63606	0.000277	0.025433
ENSG00000249661	TNRC18P1	4.18725364	-1.921707456	0.528412	-3.63676	0.000276	0.025433
ENSG00000218227	AC136632.1	60.5531005	-1.610799685	0.442809	-3.63768	0.000275	0.025433
ENSG00000144820	ADGRG7	148.449404	4.33104892	1.192787	3.631032	0.000282	0.025842
ENSG00000222057	RNU4-62P	4.79309956	-2.525394685	0.696161	-3.6276	0.000286	0.026096
ENSG00000243766	HOTTIP	94.9825193	5.119680533	1.411934	3.626006	0.000288	0.026166
ENSG00000160219	GAB3	315.115907	-1.625816119	0.448708	-3.62333	0.000291	0.026346
ENSG00000115507	OTX1	100.734909	2.153605643	0.595073	3.619063	0.000296	0.02641
ENSG00000267374	AC016205.1	30.1777681	2.624000386	0.725041	3.619106	0.000296	0.02641
ENSG00000249853	HS3ST5	37.2977677	3.554226385	0.981821	3.620034	0.000295	0.02641
ENSG00000205847	OR7E91P	27.932587	4.1027078	1.133898	3.618233	0.000297	0.02641
ENSG00000148826	NKX6-2	42.3895056	5.801032414	1.602475	3.620045	0.000295	0.02641
ENSG00000006555	TTC22	1404.44061	1.373650687	0.380085	3.614062	0.000301	0.026711
ENSG00000117650	NEK2	410.693844	1.995882467	0.552336	3.613531	0.000302	0.026711
ENSG00000265096	C1QTNF1-AS1	9.79585121	-2.544576493	0.704477	-3.61201	0.000304	0.026763
ENSG00000267040	AC027097.1	71.9409944	-1.252512361	0.346992	-3.60963	0.000307	0.026763
ENSG00000198088	NUP62CL	158.104496	1.654458523	0.458359	3.609527	0.000307	0.026763
ENSG00000251191	LINC00589	13.7964847	3.260893097	0.904915	3.603536	0.000314	0.027205
ENSG00000241359	SYNPR-AS1	30.5666196	2.969700335	0.824898	3.600082	0.000318	0.027477
ENSG00000086300	SNX10	942.393187	-1.526374137	0.424177	-3.59844	0.00032	0.027511
ENSG00000100994	PYGB	15693.8289	1.589512193	0.441772	3.59804	0.000321	0.027511
ENSG00000268849	SIGLEC22P	4.34410387	-2.101954661	0.585153	-3.59215	0.000328	0.02796
ENSG00000128408	RIBC2	72.1011124	2.154794991	0.599868	3.592114	0.000328	0.02796
ENSG00000160883	HK3	462.010269	-2.339047302	0.652157	-3.58663	0.000335	0.02827
ENSG00000005844	ITGAL	1163.40627	-2.324067813	0.648041	-3.5863	0.000335	0.02827
ENSG00000269072	AC063977.6	3.00095994	-2.127335015	0.593115	-3.58672	0.000335	0.02827
ENSG00000122986	HVCN1	434.20858	-1.79629802	0.501177	-3.58416	0.000338	0.02827
ENSG00000180539	C9orf139	42.0573063	-1.658490655	0.462575	-3.58534	0.000337	0.02827
ENSG00000231369	Z97353.1	5.40890258	-1.171981088	0.327066	-3.58332	0.000339	0.02827
ENSG00000261762	AC027228.2	67.5960408	2.145347178	0.598582	3.584052	0.000338	0.02827
ENSG00000185499	MUC1	40678.3358	2.479915109	0.692423	3.581501	0.000342	0.028377
ENSG00000139874	SSTR1	658.794366	3.057031881	0.854278	3.578498	0.000346	0.028613
ENSG00000165807	PPP1R36	239.727459	1.637226186	0.457872	3.575732	0.000349	0.028826
ENSG00000143776	CDC42BPA	5765.75353	1.047582612	0.293072	3.574492	0.000351	0.028871
ENSG00000279427	AC007490.1	48.2741352	2.283917265	0.639244	3.572841	0.000353	0.028962
ENSG00000112799	LY86	484.798192	-1.997894616	0.559503	-3.57084	0.000356	0.029002

ENSG00000019102	VSIG2	4328.11783	2.769978124	0.775557	3.571599	0.000355	0.029002
ENSG00000260963	AC026462.3	18.5531369	3.413162758	0.956229	3.569397	0.000358	0.02907
ENSG00000154016	GRAP	70.1939853	-1.856059422	0.520192	-3.56803	0.00036	0.029119
ENSG00000259485	LINC02253	83.8693851	5.022111851	1.407947	3.566976	0.000361	0.029119
ENSG00000204542	C6orf15	150.580101	5.206488048	1.459825	3.566514	0.000362	0.029119
ENSG00000276842	AC023510.2	16.4172516	-2.158218693	0.605476	-3.5645	0.000365	0.029253
ENSG00000231226	TRIM31-AS1	31.9513166	2.815247367	0.790254	3.56246	0.000367	0.029364
ENSG00000172927	MYEOV	2739.87359	3.018614097	0.847476	3.561889	0.000368	0.029364
ENSG00000184060	ADAP2	522.860817	-1.342962393	0.377123	-3.56107	0.000369	0.029366
ENSG00000124635	HIST1H2BJ	91.9278684	2.542480146	0.714302	3.55939	0.000372	0.029375
ENSG00000163993	S100P	13512.9992	3.352472117	0.941764	3.55978	0.000371	0.029375
ENSG00000086159	AQP6	81.5301899	3.265294811	0.917778	3.557825	0.000374	0.029461
ENSG00000175832	ETV4	1776.24751	2.09262378	0.588541	3.555614	0.000377	0.02962
ENSG00000256427	AC010175.1	3.83426563	-2.41774937	0.680519	-3.5528	0.000381	0.029667
ENSG00000115956	PLEK	1015.45659	-2.131543153	0.600011	-3.55251	0.000382	0.029667
ENSG00000007129	CEACAM21	96.0423827	-1.918287957	0.540173	-3.55125	0.000383	0.029667
ENSG00000205420	KRT6A	3655.21989	4.644209301	1.30688	3.553662	0.00038	0.029667
ENSG00000145384	FABP2	33.7798637	5.624974949	1.583741	3.551702	0.000383	0.029667
ENSG00000128815	WDFY4	966.285981	-2.525338894	0.712083	-3.54641	0.000391	0.030128
ENSG00000162482	AKR7A3	1441.65187	2.624013457	0.740322	3.544423	0.000393	0.030266
ENSG00000267416	AC025048.4	19.7540203	-1.496672144	0.423187	-3.53667	0.000405	0.030985
ENSG00000163624	CDS1	1939.79548	1.38842794	0.392574	3.536727	0.000405	0.030985
ENSG00000153898	MCOLN2	150.825575	-2.218975431	0.627846	-3.53427	0.000409	0.031026
ENSG00000105383	CD33	187.103393	-1.747780565	0.494543	-3.53413	0.000409	0.031026
ENSG00000280924	LINC00628	8.64740916	4.155756658	1.175934	3.534005	0.000409	0.031026
ENSG00000107099	DOCK8	1800.47676	-1.787006825	0.506011	-3.53156	0.000413	0.031061
ENSG00000149260	CAPN5	7187.72578	1.932250128	0.547163	3.531399	0.000413	0.031061
ENSG00000224259	LINC01133	1313.84521	3.048154554	0.862881	3.53253	0.000412	0.031061
ENSG00000183542	KLRC4	3.66722076	-2.853800395	0.8107	-3.52017	0.000431	0.031151
ENSG00000164935	DCSTAMP	76.9349434	-2.305810389	0.653953	-3.52596	0.000422	0.031151
ENSG00000134061	CD180	388.269146	-2.260347309	0.641463	-3.52374	0.000426	0.031151
ENSG00000122122	SASH3	1112.37723	-2.17034647	0.616128	-3.52256	0.000427	0.031151
ENSG00000010671	BTK	557.623883	-2.139347108	0.606751	-3.5259	0.000422	0.031151
ENSG00000269800	PLEKHA3P1	8.35815314	-1.887392014	0.53521	-3.52645	0.000421	0.031151
ENSG00000279377	AC003973.3	66.5666162	-1.878629367	0.533239	-3.52306	0.000427	0.031151
ENSG00000227954	TARID	22.9834313	-1.80695057	0.513067	-3.52186	0.000429	0.031151
ENSG00000258539	AC068896.1	10.8448929	-1.766195971	0.500716	-3.52734	0.00042	0.031151
ENSG00000152229	PSTPIP2	490.333228	-1.572451061	0.446153	-3.52446	0.000424	0.031151
ENSG00000137269	LRRC1	1549.43778	1.058690512	0.300754	3.520126	0.000431	0.031151
ENSG00000260328	AC104024.2	29.190294	2.580813988	0.733011	3.520839	0.00043	0.031151
ENSG00000258689	LINC01269	28.8130227	2.798282759	0.793611	3.526011	0.000422	0.031151
ENSG00000179674	ARL14	1565.0797	2.924576423	0.828994	3.527862	0.000419	0.031151
ENSG00000265206	AC004687.1	129.663471	-2.890536586	0.822073	-3.51616	0.000438	0.031369
ENSG00000101445	PPP1R16B	836.08883	-2.141533755	0.609069	-3.51608	0.000438	0.031369
ENSG00000172818	OVOL1	446.872613	2.599274827	0.739036	3.517117	0.000436	0.031369
ENSG00000096996	IL12RB1	261.507205	-1.723811224	0.490743	-3.51266	0.000444	0.031688
ENSG00000166897	ELFN2	440.353417	2.52042626	0.717868	3.510991	0.000446	0.0318
ENSG00000226491	FTOP1	16.4962072	-1.519760576	0.433042	-3.5095	0.000449	0.031892
ENSG00000140678	ITGAX	1782.07522	-1.728006175	0.492639	-3.50765	0.000452	0.032026
ENSG00000203711	C6orf99	28.4114148	2.013195467	0.574196	3.506114	0.000455	0.032124
ENSG00000106089	STX1A	1929.47905	1.822397882	0.52006	3.50421	0.000458	0.032267
ENSG00000179869	ABCA13	141.911351	2.744304422	0.783558	3.502362	0.000461	0.032327
ENSG00000232498	AL136987.1	8.59243124	5.638181162	1.609863	3.502274	0.000461	0.032327
ENSG00000011426	ANLN	1351.55435	2.125387502	0.60807	3.495299	0.000474	0.033006
ENSG00000171243	SOSTDC1	157.20821	3.616607123	1.034684	3.495373	0.000473	0.033006
ENSG00000238113	LINC01410	55.7018811	-1.762980991	0.504757	-3.49273	0.000478	0.033236
ENSG00000136542	GALNT5	2730.28746	2.61424653	0.748831	3.491102	0.000481	0.03335
ENSG00000230937	MIR205HG	133.28201	5.724753783	1.641961	3.486535	0.000489	0.033835
ENSG00000248714	AC091180.2	3.77702911	-1.9842435	0.569465	-3.4844	0.000493	0.033862
ENSG00000225342	AC079630.1	21.0603124	-1.786809467	0.512735	-3.48486	0.000492	0.033862
ENSG00000110031	LPXN	976.391637	-1.403507409	0.402821	-3.48419	0.000494	0.033862
ENSG00000162078	ZG16B	1809.99454	2.792551341	0.802257	3.480869	0.0005	0.034195
ENSG00000133048	CHI3L1	1788.12679	-2.622722653	0.754923	-3.47416	0.000512	0.034677

ENSG00000167083	GNGT2	90.2171681	-1.531135611	0.440725	-3.47413	0.000513	0.034677
ENSG00000056558	TRAF1	979.797135	-1.298258145	0.37364	-3.47463	0.000512	0.034677
ENSG00000206069	TMEM211	19.4043564	4.010392693	1.154222	3.474542	0.000512	0.034677
ENSG00000277268	AC243773.2	18.8516189	6.774176485	1.950183	3.47361	0.000514	0.034677
ENSG00000260220	CCDC187	92.6366246	2.568977494	0.740223	3.470544	0.000519	0.034984
ENSG00000107159	CA9	3657.86144	3.593013687	1.036911	3.465112	0.00053	0.035515
ENSG00000146054	TRIM7	548.249771	2.361475046	0.681639	3.464409	0.000531	0.035516
ENSG00000100027	YPEL1	112.011056	-1.132309297	0.326953	-3.46322	0.000534	0.035582
ENSG00000197465	GYPE	21.6416548	-1.833060604	0.530083	-3.45806	0.000544	0.036178
ENSG00000168078	PBK	242.662634	1.831933258	0.530096	3.455849	0.000549	0.036383
ENSG00000095539	SEMA4G	2041.34639	1.831754408	0.530694	3.451619	0.000557	0.036833
ENSG00000275216	AL161431.1	339.539485	5.123411063	1.484548	3.451158	0.000558	0.036833
ENSG00000240216	CPHL1P	62.7352668	3.837058837	1.112414	3.449308	0.000562	0.036965
ENSG00000005073	HOXA11	66.5872699	4.026565311	1.167518	3.448825	0.000563	0.036965
ENSG00000169442	CD52	1670.62611	-2.377883268	0.690063	-3.44589	0.000569	0.037262
ENSG00000171608	PIK3CD	1150.62236	-1.57255824	0.456485	-3.44493	0.000571	0.037262
ENSG00000110723	EXPH5	536.50137	1.374471606	0.399019	3.444628	0.000572	0.037262
ENSG00000272980	Z94721.2	7.08552298	-1.64182157	0.476852	-3.44304	0.000575	0.037294
ENSG00000227038	GTF2IP7	30.3363918	2.457746773	0.713784	3.443263	0.000575	0.037294
ENSG00000272468	AL021807.1	26.6338161	2.817153048	0.818406	3.442246	0.000577	0.037311
ENSG00000174791	RIN1	1223.55773	1.446239215	0.420386	3.440267	0.000581	0.037399
ENSG00000164379	FOXQ1	1811.25958	2.088594868	0.607	3.440847	0.00058	0.037399
ENSG00000148600	CDHR1	42.8642167	-2.522909862	0.733735	-3.43845	0.000585	0.037439
ENSG00000276231	PIK3R6	158.290422	-1.416779483	0.412011	-3.4387	0.000585	0.037439
ENSG00000104413	ESRP1	4052.89176	1.594523594	0.463798	3.437971	0.000586	0.037439
ENSG00000101842	VSIG1	3192.92748	3.667945324	1.067525	3.435932	0.000591	0.037566
ENSG00000260284	TPSP2	43.5413947	4.253233299	1.237943	3.435726	0.000591	0.037566
ENSG00000163508	EOMES	98.2139187	-2.557173361	0.745019	-3.43236	0.000598	0.037577
ENSG00000270164	LINC01480	78.7282138	-2.020813556	0.588309	-3.43495	0.000593	0.037577
ENSG00000236901	MIR600HG	216.963153	-1.973719164	0.574983	-3.43266	0.000598	0.037577
ENSG00000171346	KRT15	1068.12931	2.645786902	0.770737	3.4328	0.000597	0.037577
ENSG00000181631	P2RY13	196.280209	-2.175286076	0.634047	-3.4308	0.000602	0.037703
ENSG00000135773	CAPN9	956.134985	3.374028239	0.983872	3.429335	0.000605	0.037815
ENSG00000204839	MROH6	2045.6906	2.289057944	0.66786	3.427454	0.000609	0.037987
ENSG00000205268	PDE7A	1523.87065	-1.376342252	0.401999	-3.42374	0.000618	0.038417
ENSG00000280153	AC133065.6	301.581333	-1.828705583	0.534346	-3.42233	0.000621	0.038524
ENSG00000111701	APOBEC1	261.08098	3.793550387	1.108677	3.421691	0.000622	0.038524
ENSG00000186583	SPATC1	20.2885481	-2.123598157	0.620777	-3.42087	0.000624	0.038548
ENSG00000249464	LINC01091	110.525099	2.312993325	0.676279	3.420177	0.000626	0.038551
ENSG00000170786	SDR16C5	1804.87086	2.777175476	0.812143	3.419566	0.000627	0.038551
ENSG00000162543	UBXN10	887.463119	1.757017269	0.51396	3.41859	0.000629	0.038598
ENSG00000086288	NME8	19.7779347	-1.731870767	0.506973	-3.4161	0.000635	0.038704
ENSG00000077152	UBE2T	428.134058	1.448907614	0.424163	3.415919	0.000636	0.038704
ENSG00000105219	CNTD2	51.8228197	3.351568539	0.981081	3.4162	0.000635	0.038704
ENSG00000101213	PTK6	2631.09265	2.293328706	0.672086	3.412255	0.000644	0.039137
ENSG00000235897	TM4SF19-AS1	19.4526116	-1.509740978	0.442734	-3.41004	0.00065	0.039198
ENSG00000198380	GFPT1	6954.4109	1.028760516	0.301739	3.409441	0.000651	0.039198
ENSG00000187837	HIST1H1C	2357.36836	2.040153906	0.598399	3.409356	0.000651	0.039198
ENSG00000272068	AL365181.2	290.484515	2.994968151	0.878472	3.409294	0.000651	0.039198
ENSG00000094804	CDC6	524.934084	1.635121345	0.479719	3.408501	0.000653	0.039221
ENSG00000236876	TMSB4XP1	7.49150452	-1.544332506	0.453585	-3.40473	0.000662	0.039591
ENSG00000139800	ZIC5	24.8232584	5.642055655	1.657148	3.404679	0.000662	0.039591
ENSG00000134762	DSC3	272.116908	3.305473292	0.971099	3.403849	0.000664	0.039621
ENSG00000162460	TMEM82	27.109296	3.80449375	1.117948	3.403105	0.000666	0.039638
ENSG00000156453	PCDH1	8046.36279	1.396316069	0.41048	3.401667	0.00067	0.039756
ENSG00000101336	HCK	1184.77617	-1.648677488	0.485143	-3.39833	0.000678	0.040152
ENSG00000213075	RPL31P11	2.89894775	-2.261867782	0.66583	-3.39706	0.000681	0.040156
ENSG00000092607	TBX15	263.608113	2.84339012	0.836961	3.397281	0.000681	0.040156
ENSG00000140284	SLC27A2	286.429628	2.242737089	0.660433	3.395861	0.000684	0.040241
ENSG00000226690	AC013470.2	5.11591296	4.887289193	1.439637	3.394807	0.000687	0.040306
ENSG00000164078	MST1R	4222.16162	2.141018928	0.631679	3.389411	0.0007	0.041015
ENSG00000115523	GNLY	235.21983	-1.989780853	0.587353	-3.38771	0.000705	0.041141
ENSG00000198734	F5	3369.51719	2.716727701	0.802026	3.387332	0.000706	0.041141

ENSG00000261465	AC099518.4	8.34335748	2.310793512	0.682318	3.38668	0.000707	0.041147
ENSG00000136286	MYO1G	684.897616	-1.812430155	0.535723	-3.38315	0.000717	0.041587
ENSG00000270379	HEATR9	6.29980313	-2.2557178	0.667325	-3.38024	0.000724	0.041676
ENSG00000273062	AL449106.1	17.4847665	-1.482566816	0.438683	-3.37959	0.000726	0.041676
ENSG00000213371	NAP1L1P3	6.5326642	-1.142942388	0.33803	-3.38119	0.000722	0.041676
ENSG00000227155	AL161725.1	14.6959435	-1.929267643	0.571775	-3.37417	0.00074	0.042124
ENSG00000204991	SPIRE2	1472.63827	2.038583252	0.604171	3.374183	0.00074	0.042124
ENSG00000250271	AC068647.2	20.2602533	4.437077255	1.314612	3.375198	0.000738	0.042124
ENSG00000267369	AC015911.7	51.8147896	-1.99339354	0.591564	-3.3697	0.000753	0.042636
ENSG00000233217	MROH3P	181.340608	3.203930561	0.950998	3.369019	0.000754	0.042636
ENSG00000123329	ARHGAP9	752.735485	-1.952923108	0.579811	-3.36821	0.000757	0.042669
ENSG00000196405	EVL	3370.00816	-1.39247419	0.413597	-3.36674	0.000761	0.042804
ENSG00000186517	ARHGAP30	1723.35378	-1.686417305	0.501217	-3.36465	0.000766	0.043037
ENSG00000166866	MYO1A	969.27542	3.154725828	0.937998	3.363255	0.00077	0.043161
ENSG00000104951	IL4I1	476.060348	-2.045485466	0.608613	-3.3609	0.000777	0.043438
ENSG00000185015	CA13	602.209351	1.457663617	0.43403	3.35844	0.000784	0.043732
ENSG00000111860	CEP85L	352.931261	-1.186925963	0.354165	-3.35134	0.000804	0.044387
ENSG00000176920	FUT2	2311.36809	1.923233578	0.573965	3.350786	0.000806	0.044387
ENSG00000101447	FAM83D	567.529914	2.228968763	0.664965	3.352008	0.000802	0.044387
ENSG00000167755	KLK6	3327.73254	3.606747997	1.075468	3.353655	0.000798	0.044387
ENSG00000267287	AC068473.3	22.2718612	-1.864386109	0.556926	-3.34764	0.000815	0.044711
ENSG00000262714	AC007342.5	39.0626488	2.826037343	0.844198	3.347602	0.000815	0.044711
ENSG00000135898	GPR55	40.3375702	-2.187969992	0.654003	-3.3455	0.000821	0.044767
ENSG00000265743	AC138207.5	33.4137291	-1.407301856	0.420619	-3.34579	0.00082	0.044767
ENSG00000110244	APOA4	143.162102	7.120313761	2.128231	3.345649	0.000821	0.044767
ENSG00000196329	GIMAP5	102.192597	-2.113321656	0.632265	-3.34246	0.00083	0.045166
ENSG00000223813	AC007255.1	53.0321115	1.703069004	0.509621	3.341833	0.000832	0.045174
ENSG00000102445	RUBCNL	327.530553	-1.994262409	0.596977	-3.3406	0.000836	0.045186
ENSG00000189238	LINC00943	7.75412261	-2.133539798	0.639664	-3.33541	0.000852	0.04541
ENSG00000224968	LINC01645	3.78495247	-2.117496783	0.635166	-3.33377	0.000857	0.04541
ENSG00000015285	WAS	828.496173	-1.795871547	0.539328	-3.32983	0.000869	0.04541
ENSG00000268316	AC006272.1	3.37452835	-1.682204137	0.504445	-3.33476	0.000854	0.04541
ENSG00000274712	AC005332.7	105.52057	-1.41482331	0.424383	-3.33383	0.000857	0.04541
ENSG00000150867	PIP4K2A	2230.46659	-1.073039063	0.322276	-3.32957	0.00087	0.04541
ENSG00000121057	AKAP1	4055.5721	1.067282323	0.320318	3.33195	0.000862	0.04541
ENSG00000213853	EMP2	5096.33425	1.201370596	0.360498	3.332529	0.000861	0.04541
ENSG00000079385	CEACAM1	3865.42623	1.862364387	0.559141	3.330759	0.000866	0.04541
ENSG00000226330	AL606489.1	35.4696022	1.954036725	0.586574	3.331272	0.000865	0.04541
ENSG00000204335	SP5	110.59096	2.678422223	0.80419	3.330584	0.000867	0.04541
ENSG00000099834	CDHR5	2276.28768	2.788007228	0.837283	3.329828	0.000869	0.04541
ENSG00000132821	VSTM2L	3068.41807	2.79451631	0.838826	3.331461	0.000864	0.04541
ENSG00000188100	FAM25A	5.7150008	5.041744381	1.512714	3.332913	0.000859	0.04541
ENSG00000113303	BTNL8	510.491986	3.565838892	1.071601	3.327582	0.000876	0.045577
ENSG00000231324	AP000696.1	13.0911516	4.346753439	1.30634	3.32743	0.000877	0.045577
ENSG00000108691	CCL2	2088.27563	-2.181517025	0.656428	-3.32331	0.00089	0.045697
ENSG00000265798	AC138207.6	11.0862376	-1.501185233	0.451548	-3.32453	0.000886	0.045697
ENSG00000280194	AD000864.1	29.1940613	-1.341574148	0.403554	-3.32439	0.000886	0.045697
ENSG00000006611	USH1C	4288.41362	1.88569264	0.567791	3.321105	0.000897	0.045697
ENSG00000175318	GRAMD2A	193.738708	1.992512143	0.600041	3.320629	0.000898	0.045697
ENSG00000196890	HIST3H2BB	53.2317536	2.469743331	0.74257	3.325938	0.000881	0.045697
ENSG00000167644	C19orf33	5348.37311	2.474552482	0.74507	3.321235	0.000896	0.045697
ENSG00000179148	ALOXE3	43.9387698	2.499563568	0.752433	3.321974	0.000894	0.045697
ENSG00000239093	snoU13	8.27508527	3.15286829	0.949111	3.321917	0.000894	0.045697
ENSG00000166589	CDH16	38.544366	3.676392208	1.106207	3.323422	0.000889	0.045697
ENSG00000240476	LINC00973	28.7490385	4.595089068	1.383587	3.321141	0.000897	0.045697
ENSG00000185482	STAC3	235.958217	-1.133273021	0.341529	-3.31823	0.000906	0.045732
ENSG00000130762	ARHGEF16	3058.30489	1.598908313	0.481824	3.318447	0.000905	0.045732
ENSG00000124107	SLPI	9912.17224	2.257826666	0.680397	3.318396	0.000905	0.045732
ENSG00000198835	GJC2	383.563972	2.409049492	0.725689	3.31967	0.000901	0.045732
ENSG00000239961	LILRA4	60.2482752	-2.879821231	0.868023	-3.31768	0.000908	0.045734
ENSG00000153292	ADGRF1	1694.15126	2.633483328	0.793908	3.317113	0.00091	0.045739
ENSG00000188820	FAM26F	253.641079	-1.971132999	0.594603	-3.31504	0.000916	0.045902
ENSG00000138756	BMP2K	430.123567	-1.086720677	0.327972	-3.31346	0.000921	0.046073

ENSG00000188536	HBA2	395.707208	-3.233727938	0.977562	-3.30795	0.00094	0.046779
ENSG00000123338	NCKAP1L	1823.57083	-1.873957156	0.566445	-3.30828	0.000939	0.046779
ENSG00000204121	ECEL1P1	12.6716589	4.694755964	1.419386	3.307596	0.000941	0.046779
ENSG00000227191	TRGC2	57.3685509	-2.225207329	0.673197	-3.30543	0.000948	0.046962
ENSG00000160321	ZNF208	49.2295945	-1.646522093	0.498051	-3.30593	0.000947	0.046962
ENSG00000121957	GPSM2	523.540024	1.1487345	0.34838	3.297362	0.000976	0.047876
ENSG00000174607	UGT8	1391.54334	1.594161002	0.483201	3.299167	0.00097	0.047876
ENSG00000143375	CGN	7268.92387	1.629682745	0.494186	3.297708	0.000975	0.047876
ENSG00000258077	AC078923.1	9.80606574	3.827399055	1.16041	3.298317	0.000973	0.047876
ENSG00000253258	AC068228.2	4.3697963	4.652986634	1.411059	3.297514	0.000975	0.047876
ENSG00000242747	AC090515.1	5.3125842	-1.537223347	0.466485	-3.29533	0.000983	0.048042
ENSG00000224137	LINC01857	49.0407035	-2.945545281	0.894504	-3.29294	0.000991	0.048141
ENSG00000143119	CD53	2706.1744	-1.941983312	0.589773	-3.29276	0.000992	0.048141
ENSG00000234964	FABP5P7	5.35885771	-1.673443714	0.508398	-3.2916	0.000996	0.048141
ENSG00000254827	SLC22A18AS	194.9412	1.857643721	0.564162	3.292746	0.000992	0.048141
ENSG00000118194	TNNT2	156.511118	2.610094605	0.792839	3.292085	0.000994	0.048141
ENSG00000167964	RAB26	563.950396	2.640644534	0.802087	3.292219	0.000994	0.048141
ENSG00000244468	AC093001.1	6.64385339	5.263370047	1.602039	3.285419	0.001018	0.049119
ENSG00000213279	Z97192.2	11.0147348	-1.730672469	0.526887	-3.28471	0.001021	0.049151
ENSG00000188060	RAB42	207.751694	-1.640880658	0.499821	-3.28294	0.001027	0.049188
ENSG00000147676	MAL2	13324.195	1.685358114	0.513296	3.283405	0.001026	0.049188
ENSG00000161643	SIGLEC16	36.4030319	-1.878343972	0.572298	-3.28211	0.00103	0.049242
ENSG00000158517	NCF1	209.772933	-2.16561013	0.660109	-3.28069	0.001036	0.049276
ENSG00000135596	MICAL1	3059.99244	-1.042356466	0.317816	-3.27975	0.001039	0.049276
ENSG00000170522	ELOVL6	1152.05549	1.335620712	0.407348	3.27882	0.001042	0.049276
ENSG00000175164	ABO	1864.17373	2.275605964	0.693519	3.281245	0.001033	0.049276
ENSG00000123843	C4BPB	702.372719	2.664791673	0.812657	3.279111	0.001041	0.049276
ENSG00000254548	AC105219.2	13.0067685	3.79795819	1.158093	3.279494	0.00104	0.049276
ENSG00000126882	FAM78A	559.364829	-1.704631343	0.520172	-3.27706	0.001049	0.049406
ENSG00000154133	ROBO4	940.086206	-1.158837004	0.353603	-3.27723	0.001048	0.049406
ENSG00000164129	NPY5R	11.5031536	-2.963135483	0.905044	-3.27402	0.00106	0.049513
ENSG00000131042	LILRB2	428.874969	-1.763764462	0.538402	-3.27593	0.001053	0.049513
ENSG00000175866	BAIAP2	3044.25548	1.312594002	0.400797	3.274958	0.001057	0.049513
ENSG00000137460	FHDC1	898.829474	1.526157491	0.46616	3.273895	0.001061	0.049513
ENSG00000211974	AC245369.1	69.4594686	4.393470804	1.341719	3.274509	0.001058	0.049513
ENSG00000197872	FAM49A	812.24303	-1.478459649	0.45187	-3.27187	0.001068	0.049602
ENSG00000237523	LINC00857	237.760665	1.787683432	0.546285	3.27244	0.001066	0.049602
ENSG00000047597	XK	311.905072	2.043372237	0.624455	3.272251	0.001067	0.049602
ENSG00000121075	TBX4	11.9140423	3.653151567	1.116782	3.271141	0.001071	0.049641
ENSG00000170608	FOXA3	2175.86884	2.152692635	0.658565	3.268764	0.00108	0.049838
ENSG00000255545	AP004608.1	192.464306	3.039462611	0.929736	3.269167	0.001079	0.049838
ENSG00000280362	AC084759.3	24.5304416	4.038152044	1.23547	3.268515	0.001081	0.049838

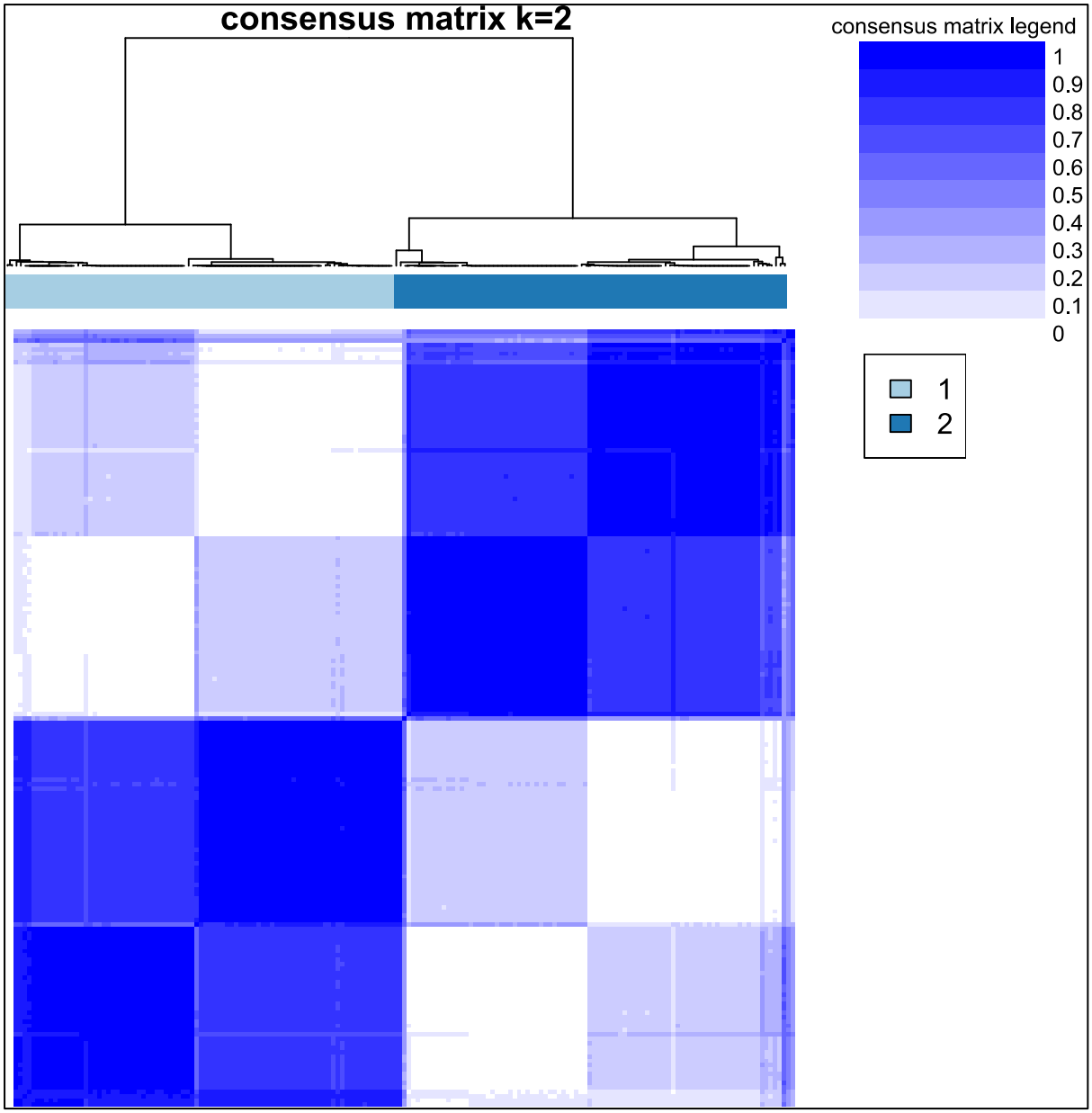

Appendix figure 1: Result of consensus clustering analysis. Heatmap of the consensus matrix M *(K)* for K = 2 which is the optimal number of clusters, cluster 1 (n=88 patients) and cluster2 (n= 89 patients) with clustering consensus values 0.8774 and 0.8452, respectively. Consensus values range from 0 (never clustered together) to 1 (always clustered) marked by white to dark blue. FPKMs of the top eight significantly prognostic genes for the 177 PDAC tumour samples were used for the analysis applying the parameters mentioned in material and methods.